Master of science dissertation
in medical radiation physics

Evaluation of current quality assurance (QA) system for volumetric modulated arc therapy (VMAT) by studying the impact of introduced errors

Marcus Krantz

Supervisors: Claus F. Behrens PhD, David Sjöström, Rickard Ottosson and Maria Sjölin

The work has been performed at the
department of oncology
Copenhagen University hospital, Herlev, Denmark

Medical radiation physics
Clinical sciences, Lund
Lund University, 2010

Felkällor vid strålbehandling – vilka konsekvenser uppstår?

Strålbehandling är en vanlig behandlingsform vid cancer. Röntgenstrålning med hög energi från en strålningsapparat (linjäraccelerator) låter man träffa behandlingsområdet, med syftet att döda cancercellerna. Strålningen påverkar även friska celler, men målet är att spara normal vävnad så mycket som möjligt. Av den anledningen måste stråldosen till frisk vävnad minimeras med ändå ge en hög stråldos till tumörcellerna.

Vid Herlev universitetssjukhus används en ny avancerad rotationsteknik (RapidArc®) vid strålbehandling av cancer. Tekniken är ett system som bestrålar patienten under en 360° rotation där blylameller, stråldoshastighet och strålkällans hastighet runt patienten är varierbara. Strålbehandling med den nya rotationstekniken syftar till att öka stråldosen till tumören men samtidigt minska risken för skador på den friska vävnaden samt förkorta behandlingstiden. På grund av teknikens komplexitet, behövs ökad kunskap gällande effekten av eventuella felkällor hos linjäracceleratorn. Ökad kännedom krävs också om eller när eventuella felkällor vid bestrålning kan upptäckas med hjälp av en avancerad mätmetod och vilken betydelse felkällorna kan ha för patienten.

Som en del av kvalitetssäkringssystemet kontrollerar man den planerade fördelningen av absorberad dos till patienten med hjälp av mätningar. Ett sätt att öka kunskapen kring osäkerheter i nuvarande kvalitetssäkringssystem är att systematiskt bygga in medvetna ”fel” som simulerar bristerna hos linjäracceleratorn, som därmed skulle kunna leda till sämre behandling.

Denna studie syftade till att öka kunskapen om eller när eventuella fel vid strålbehandling kan upptäckas med hjälp av en befintlig och specifik mätmetod och vilka konsekvenser osäkerheterna kan innebära för patienten. Samt skulle utredning ske huruvida oberoende noggranna stråldosberäkningar kan vara en del av nuvarande kvalitetssäkringssystem. För- och nackdelar med de olika utvärderingsmetoderna undersöktes också.

De flesta inbyggda fel var möjliga att upptäcka och större delen av de fel som inte kunde upptäckas innebar endast försumbara konsekvenser för patienten. Några av de inbyggda felen, som inte tydligt kunde påvisas med den befintliga mätmetoden, visade sig dock med noggranna stråldosberäkningar ge effekter, av varierande grad, i dosplanerna.

Den undersökta mätmetoden var mycket känslig för de inbyggda felen eftersom mätresultat kan utvärderas på flera olika sätt. Oberoende noggranna stråldosberäkningar kan användas för att kontrollera olika dosplaners kvalitet och skulle därmed kunna vara en del av nuvarande kvalitetssäkringssystem.

Handledare: **Claus F. Behrens, David Sjöström, Rickard Ottosson och Maria Sjölin.**
Examensarbete på 30 hp i medicinsk strålningsfysik
Avdelningen för medicinsk strålningsfysik, Lunds universitet
Arbetet utfördes på universitetssjukhuset i Herlev, Danmark

Evaluation of current quality assurance (QA) system for volumetric modulated arc therapy (VMAT) by studying the impact of introduced errors

Introduction: Currently, patient specific dosimetric measurements on diode arrays such as Delta$^{4®}$ (ScandiDos AB) is a part of standard quality assurance (QA) for RapidArc® (RA) at Herlev University hospital. However, a standing issue is the interpretation of the results from dosimetric measurements into consequences in the delivered absorbed dose to the patient. Furthermore, measurements are time consuming. Thus, alternative QA systems are desirable for RA delivery. The aim of this study was to investigate (a) the impact of introduced known errors, (b) whether clinically important errors are detectable by the current QA system and (c) the benefits and drawbacks of dosimetric measurements and Monte Carlo (MC) absorbed dose calculations for RA QA.

Materials and methods: RA beam delivery was performed using a Varian Clinac 2300 iX for nine prostate treatment plans and one H&N treatment plan with and without introduced errors. The DICOM plan files were edited and systematic errors were introduced by shifting the position of one of the MLC banks. Systematic errors introduced were ±0.5 mm, ±1.0 mm, ±1.5 mm and ±2.0 mm. The minus and plus signs corresponds to the direction that results in larger and smaller aperture, respectively. The erroneous treatment plans were calculated in Eclipse™ using the analytical anisotropic algorithm (AAA) and the planes were subsequently measured employing the Delta$^{4®}$ diode array. The impact of erroneous treatment plans was evaluated in terms of clinical importance by comparison of the planning target volume enclosed by ≥95% ($PTV_{95\%}$) of the prescribed absorbed dose, the volume enclosed by ≥95% and ≥105% of the prescribed absorbed dose ($V_{95\%}$, $V_{105\%}$). A qualitative evaluation of calculated reference and erroneous treatment plans were carried out in terms of 2D percental absorbed dose difference with the objective to visualize the impact of introduced errors. Delivered absorbed dose distributions were evaluated using gamma analysis as built into the Delta$^{4®}$ software with acceptance criteria set to 3% dose difference/3 mm distance-to-agreement. Furthermore, dose volume histograms were evaluated for all treatment plans both in Eclipse™ and the Delta$^{4®}$ software's. All treatment plans were also calculated with MC as an alternative QA protocol.

Results: The results disclose that systematic errors < +1.0 mm and ≤ -1.0 mm in the investigated prostate treatment plans, are in general not detected with the Delta$^{4®}$ diode array. Moreover, not all introduced errors ≥ +1.0 mm and > -1.0 mm were detected using the gamma index distribution exclusively, but by means of the absorbed dose deviation tool, all errors were detected. Also, for the investigated H&N treatment plan the gamma evaluation failed to find the introduced errors. However, using the absorbed dose deviation tool the investigated introduced errors of +1.0 mm, or larger, were detected. Furthermore, the MC based QA protocol was able to visualize introduced errors.

Conclusions: Small changes in position of the MLC-bank could be of clinical importance and dosimetric measurements of introduced errors demonstrated that clinically important errors are not always detected with the currently used RA QA system. This study showed that small systematic errors could be visualized with MC. Thus, MC can be used as a part of RA QA system in the future.

Supervisors: **Claus F. Behrens, David Sjöström, Rickard Ottosson and Maria Sjölin.**
Degree project of 30 credits medical radiation physics, spring 2010
Department of Medical Radiation Physics, Lund University, Sweden
The work was carried out at the department of oncology, Copenhagen University hospital, Herlev, Denmark.

Acknowledgements

- First of all, I would like to thank all the people at Herlev University hospital involved in this work for their help and support.

- Special thanks to :

  - Claus F. Behrens and David Sjöström for their ideas which helped me improving my master´s dissertation.

  - Maria Sjölin for her kindness and helpfulness, showing me how to use the Delta$^{4®}$ diode array.

  - Rickard Ottosson for helping me to use MC in my study. Without him, this work would not be possible.

  - Ulf Bjelkengren for always trying to help me through my various problems.

- I would also like to acknowledge the Swedish foundations "Regementsläkaren Dr Hartelii foundation" and "Stiftelsen Skåneföreningen 1900-års mäns stipendiefond" for helping me expand this master's dissertation at Herlev University hospital and"John och Augusta Perssons stipendiestiftelse" for funding my participation at the European Society for Therapeutic Radiology and Oncology (ESTRO 29) conference in Barcelona (see abstract in Appendix 2).

- Finally, a great appreciation to my fellow course comrades. Without them my life as a student would have been less enjoyable.

Abbreviations and acronyms

2D	Two-dimensional
3D	Three-dimensional
CT	Computed tomography
DICOM	Digital imaging and communications in medicine
DTA	Distance-to-agreement
QA	Quality assurance
QC	Quality control
IMRT	Intensity modulated radiation therapy
IMAT	Intensity modulated arc therapy
VMAT	Volumetric modulated arc therapy
MLC	Multileaf collimator
MU	Monitor unit
MV	Mega voltage
PMMA	Polymethylmethacrylate
TPS	Treatment planning system
CP	Control point
PSF	Phase space file
ROI	Region of interest
DMLC	Dynamic MLC
MC	Monte Carlo
DVH	Dose volume histogram
NTCP	Normal tissue complication probability
TCP	Tumor control probability
CERR	Computational environment for radiotherapy research
AAA	Anisotropic analytical algorithm
PTV	Planning target volume
oPTV-T	Optimization planning target volume of tumor

Table of contents

Introduction

Cancer is the primary cause of death worldwide with 7.9 million deaths in year 2007 or approximately 13% of all deaths and are anticipated to continue rising with approximately 12 million deaths in 2030 (1). According to the Swedish national board of health and welfare (Socialstyrelsen), cancer is a very common disease with just over 50,000 individual's (2) diagnosed with cancer in year 2008. This implies that cancer is the second most common cause of death in Sweden with more than 22,000 deaths per year (2). Amongst men, prostate cancer is the most common cancer corresponding to 33% of the male cases (2). By estimate, one third of the population will be diagnosed cancer through their lifetime (3). In many years, radiotherapy has been an important modality for cancer treatment and it is applied in nearly half of all cancer treatments (4). The main purposes of cancer treatment are to cure, relieve patients from pain and help to increase the quality of life. Primary treatment techniques used to achieve these goals are radiotherapy, surgery and chemotherapy. Since improvement of radiotherapy is essential in terms of high target dose conformity and enhanced sparing of normal surrounding tissue, development of new treatment modalities in the radiotherapy community is in constant progress.

In the past decade, intensity modulated radiation therapy (IMRT) has been the technique of choice when treating cancer due to high target dose conformity and improved sparing of the normal surrounding tissues. Recently, IMRT has been delivered by arc-based techniques and the first method concerning intensity modulation and arc therapy was first proposed by Yu, 1995 where the treatment is delivered as multiple overlapping arcs and each arc consists of multiple superimposed subfields (5). This technique is referred to as intensity modulated arc therapy (IMAT), which delivers radiation with constant dose rate and gantry rotation speed. The IMAT technique was evolved by Otto, 2007 referred to as volumetric modulated arc therapy (VMAT) (6). The VMAT method enables dynamic multileaf collimators (DMLC), dose rate and gantry rotation speed over one single arc around the patient.

RapidArc® (RA) is a clinical application of rotational IMRT based on the VMAT method which is Varian Medical Systems, Inc. (Palo Alto, CA, USA) most recent development. In April 2008, RA was released for clinical use and in June 17 2009, Herlev University hospital treated their first patient using RA (7; 8). The RA method uses dynamic multileaf collimators (DMLC), dose rate and gantry rotation speed over one or several optimized arc around the patient such that these are within the capabilities of the linear accelerator (6; 8; 9; 10). This treatment technique is time efficient and produces absorbed dose distributions of high conformity (6). An introduction of a novel technique into clinical practice requires a substantial dosimetric verification to assure correct treatment delivery. This includes both quality assurance (QA) on patient specific level and general machine performance. Since RapidArc® delivery system is an exceptionally complex modality for radiotherapy treatments, a versatile QA system is indispensable (7; 9; 10; 11). Patient specific QA, however, should not substitute for machine specific and treatment planning QA intended to check the specifications and commissioning of the planning and delivery system. Then again, the results from patient specific QA can expose problems in planning or delivery systems that should be investigated with specific checks (12).

Currently, patient specific dosimetric measurements on diode arrays, 2D ion chamber arrays and film dosimetry are used for RA QA (13; 14; 15). A previous study by Korreman *et al* 2009, verified the correctness and consistency of absorbed

doses delivered with the RA method, by using the dosimetric equipment Delta$^{4®}$ (10). The gamma analysis as built into the following software was applied as a quantitative evaluation method. Another study by Bedford *et al* 2009, evaluated the Delta$^{4®}$ phantom by applying basic performance tests for linear dependency, angular sensitivity and dose rate sensitivity (16). Results were compared with other established QA methods such as ionization chambers and film dosimetry. Furthermore, recently, a study by Rangel *et al* 2010, investigated the feasibility of detecting systematic errors in the MLC leaf bank position with patient specific IMRT quality control (QC). As an evaluation, the absolute absorbed dose, the relative absorbed dose, the distance-to-agreement (DTA) and the gamma evaluation was applied (17).

However, the clinical impact of small deviations in RA beam delivery and their impact on the measurements are unknown. Moreover, a standing issue is the interpretation of the results from dosimetric measurements into consequences in the delivered absorbed dose to the patient. Herlev University hospital has implemented the possibility to perform three dimensional (3D) Monte Carlo (MC) absorbed dose calculations; with treatment planning system (TPS) generated plan files. Also, it is acceptable to use an independent 3D absorbed dose calculation as an alternative to a set of measured absorbed dose distribution (12). Therefore, a verification of the accuracy of the MC calculations is necessary.

A MC based patient specific RA QA using log files, derived from the linear accelerator was proposed by Teke *et al* 2009, where verification of both the TPS and the physical machine performance, was carried out. Comparisons between TPS and MC using TPS generated MLC files provided QC on the TPS (13). The MC method has been demonstrated to be a useful tool for radiation therapy absorbed dose calculations and MC simulations can be used to supply 3D absorbed dose information (18).

Limitations of dosimetric measurements include a lack of dosimetric precision for film dosimetry and spatial resolution issues for 2D diode arrays. Furthermore, measurements are time consuming. Thus, alternative QA systems are desirable for patient specific RA QA such as MC absorbed dose calculations.

The aim of this master dissertation was to investigate (a) the impact of introduced known errors, (b) whether clinically important errors are detectable by current QA system and (c) the benefits and drawbacks of dosimetric measurements and MC absorbed dose calculations for RA QA.

Theory

RapidArc®

RapidArc® is Varian Medical Systems most recent clinical implementation of inversely optimized arc therapy. Varian linear accelerators apply DMLC and utilize the sliding window technique for IMRT delivery to produce highly conformal coverage of the target whilst sparing normal tissues (19). The RA method is able to deliver a 2 Gy fraction faster and with fewer MU compared to IMRT without reducing the treatment quality (19).

Optimization method

The RapidArc® TPS is based on the VMAT algorithm proposed by Otto 2007 (6), where optimized treatment plans may be delivered during a single or several gantry rotations, so called arcs. Briefly, MLC positions and monitor units (MU) are integrated as optimization parameters together with an objective function based on dose volume constraints of normal tissues and the target. Constraints are imposed on MLC positions or MU weights such that the MU values and the aperture between MLC are physically possible.

For RA treatment, a single arc is divided into 177 angles named control points (CP:s), as applied in Eclipse™. The optimization method starts off with a small number of CP:s which is gradually increased until absorbed dose calculation accuracy is obtained i.e. 177 CP (Figure 1). By progressively increase the number of CP:s, an optimal solution can be obtained in a short period of time. Thus, the treatment time is reduced to 1.5 – 3 minutes for a 2 Gy fraction compared to fixed gantry IMRT (6). To maintain continuous beam delivery, constraints are also forced on dose rate variation and MLC leaf motion.

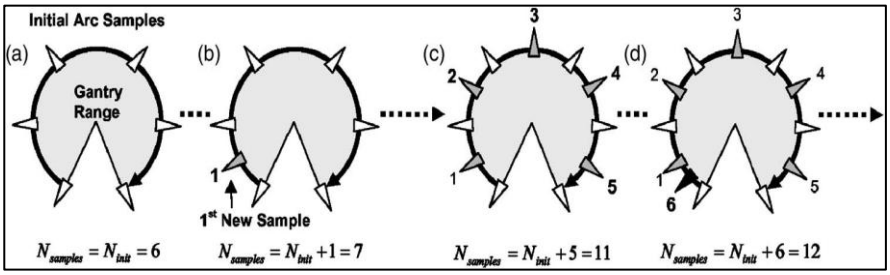

Figure 1. Continuous gantry rotation speed and MLC positions are in the beginning of the optimization represented by a sequence of static source positions which are progressively increased until dose calculation accuracy is obtained. Varian Eclipse™ applies 177 CP:s. (Image courtesy of Otto, 2007 (6)).

Varian Eclipse™ absorbed dose calculations

The anisotropic analytical algorithm (AAA v. 8.9.08) was implemented in Eclipse™ TPS which calculates the absorbed dose volumes (9). The AAA is a 3D pencil beam convolution/superposition algorithm that applies MC derived kernels. Calculation time is considerably reduced since the greater part of the convolution operators are possible to convert into analytical expressions (20). Furthermore, in a 3D region of an interaction site, AAA accounts for tissue heterogeneity anisotropically (i.e. being directionally dependent) by means of photon scatter kernels in multiple lateral directions. By superposition of electron and photon convolutions the final absorbed dose distribution is achieved.

Clinically, the AAA is sorted into two algorithms, absorbed dose calculation and dose configuration. The dose configuration algorithm determines the physical parameters required such as mean radial energy, scatter kernels and photon energy. The AAA configuration begins with selection of basic parameters from a library obtained from MC simulations of the treatment head. Subsequently, these parameters are modified to create a phase space file that is consistent with the real beam delivery applied clinically. The phase space file consist of dosimetric data such as depth dose curves, lateral profiles at various depth and output factors for open and wedged fields (20).

Separate convolution models for primary, scattered photons from beam modifiers and contaminating electrons are used as basis when absorbed dose calculations are

performed. Conventional open beams are divided into beamlets of finite size to which convolutions are employed, as well. A superposition of the absorbed dose distributions calculated with the electron and photon convolutions for every beamlet generates the final absorbed dose distribution (20; 21).

Gamma evaluation

There are several qualitative methods to evaluate absorbed dose distributions, e.g. dose volume histograms (DVHs). However, DVHs do not evaluate spatial information. Complementary, a quantitative evaluation that directly compares measured and calculated absorbed dose distribution values should be applied as a full analysis. The quantitative evaluation tools available in the Delta$^{4®}$ software for comparison of absorbed dose distributions are the DTA method, the absorbed dose deviation method and the gamma analysis method.

The absorbed dose deviation method compares the absorbed dose in the data points in the reference plan with the corresponding data points that are to be evaluated. In the Delta$^{4®}$ evaluation software the criteria for the maximum acceptable absorbed dose deviation are set regarding to the global absorbed dose and in this study the isocenter was applied. The DTA is the spatial distance between calculated and measured data points that receives the same absorbed dose. The Delta$^{4®}$ software creates an isodose surface by interpolating between the data points in the reference plan. This isodose surface is compared with measured data points. However, the Delta$^{4®}$ software only considers a maximum distance of 20 mm and the DTA is set to 20 mm if the distance to the closest point with the same absorbed dose is larger than 20 mm. A criterion for maximum acceptable DTA can be chosen manually by the user. The distance between the measured- and reference data points with the same absorbed dose must not exceed the chosen maximum DTA to pass the evaluation.

The absorbed dose deviation method is not valid in high dose gradient regions due to a small spatial error may result in a large absorbed dose difference in contrast to the DTA, that is suitable in high dose gradient regions. Therefore, DTA complements the absorbed dose deviation method for absorbed dose calculation verification. The gamma evaluation method described by Low *et al* applies two comparison tools, a direct comparison of the absorbed dose deviation and comparison of the DTA between calculated and measured absorbed dose distributions and provides a numerical index as a measure of agreement of the two dose distributions (22). The gamma evaluation method sets the criteria for both absorbed dose deviation and the distance to the closest data point in the reference plan. A gamma (γ) index is calculated for every measured dose point and if the gamma index is less than or equal to one, the dose point passes. For 2D absorbed dose distributions the two criteria, the absorbed dose deviation and the DTA, includes an ellipsoid with the surface representing the acceptance criterion (Figure 2). The ellipsoid is described by the following equation,

$$1 = \sqrt{\frac{r^2(\boldsymbol{r},\boldsymbol{r_c})}{\Delta d^2{}_M} + \frac{\delta^2(\boldsymbol{r},\boldsymbol{r_c})}{\Delta \mathrm{D}^2{}_M}} \qquad [1]$$

where $\mathrm{r}(\boldsymbol{r},\boldsymbol{r_c})$ is the spatial distance between calculated position, i.e. origin, and any arbitrary position and $\delta(\boldsymbol{r},\boldsymbol{r_c})$ is the absorbed dose deviation between the calculated position and any arbitrary position. The right hand side of equation (1) is applied when defining the gamma index,

$$\gamma(\boldsymbol{r_m}) = min\{\Gamma(\boldsymbol{r_m},\boldsymbol{r_c})\}\ \forall\ \{\boldsymbol{r_c}\} \qquad [2]$$

where

$$\Gamma(\boldsymbol{r_m}, \boldsymbol{r_c}) = \sqrt{\frac{r^2(\boldsymbol{r_m}, \boldsymbol{r_c})}{\Delta d^2{}_M} + \frac{\delta^2(\boldsymbol{r_m}, \boldsymbol{r_c})}{\Delta \mathrm{D}^2{}_M}} \quad [3]$$

$$\delta(\boldsymbol{r_m}, \boldsymbol{r_c}) = D_c(\boldsymbol{r_c}) - D_m(\boldsymbol{r}_m) \text{ and } r(\boldsymbol{r_m}, \boldsymbol{r_c}) = |\boldsymbol{r_c} - \boldsymbol{r_m}| \quad [4]$$

$\Delta \mathrm{D}_M$ is the measured absorbed dose deviation criteria at coordinate r_m, D_c is the calculated absorbed dose at coordinate r_c, Δd_M is the DTA acceptance criteria and $\Delta \mathrm{D}_M$ is the absorbed dose difference criteria. $|\boldsymbol{r_c} - \boldsymbol{r_m}|$ is the spatial distance between reference and measured dose points. According to Low *et al* 1998, (22) the pass-fail criterion is

$\gamma(\boldsymbol{r_c}) \leq 1$, calculation passes [5]

$\gamma(\boldsymbol{r_c}) > 1$, calculation fails [6]

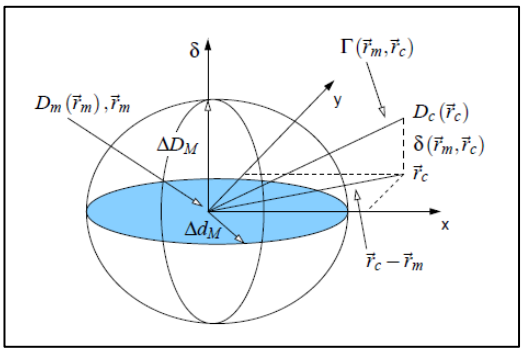

Figure 2. Geometric illustration of the Γ function for quantitative evaluation of absorbed dose distributions. The ellipsoid of acceptance is defined by the absorbed dose difference $\Delta \mathrm{D}_M$ and the DTA Δd_M. Dose points values larger than one demonstrates that gamma index do not satisfy the manually chosen criteria. Calculated and measured absorbed dose distributions are represented by D_c and D_m respectively.

Monte Carlo absorbed dose calculations

MCSIM is based on the electron gamma shower v. 4 (EGS4) code described by Nelson *et al* 1990, and has been developed at Fox Chase Cancer Center (FCCC). MCSIM includes various variance reduction techniques to speed up the Monte Carlo simulation (25; 18). The EGS4 code has been developed as a routine 3D absorbed dose calculation and treatment verification tool for radiotherapy and is the most widely used MC code in medical radiation physics (26). When using MC, the absorbed dose to medium ($\mathrm{D_M}$) is calculated in voxels representing the materials found in the body. Since the dose profiles and output factors applied in the TPS are normally generated from measurements in water phantoms, the absorbed dose calculations algorithms for photon beam radiotherapy usually report the absorbed dose to water ($\mathrm{D_W}$). Also, biological indices such as normal tissue complication probability (NTCP) and tumour control probability (TCP) are given in terms of absorbed dose to water; hence this value should be reported (27). To enable comparison between MC- and TPS algorithms the absorbed dose must be defined in the same medium. Siebers *et al* 2000, developed a method to convert $\mathrm{D_M}$ to $\mathrm{D_W}$ for photon beams using Bragg-Gray cavity theory (27). This theory relates the $\mathrm{D_M}$ to $\mathrm{D_W}$ according to

$$D_W = D_M \, S_{W,M} \quad [7]$$

The unrestricted water-to-medium mass collision stopping power ratio ($S_{W,M}$) is averaged over the energy spectrum of primary electrons $(\Phi_E)_m$. Calculation of $S_{W,M}$ is performed using

$$S_{W,M} = \int_0^{E_{max}} (\Phi_E)_m \, (S/\rho)_W \, dE \Big/ \int_0^{E_{max}} (\Phi_E)_m \, (S/\rho)_M \, dE \quad [8]$$

E_{max} is the maximum energy in the spectrum of primary electrons and $(S/\rho)_M$ and $(S/\rho)_W$ are the unrestricted mass collision stopping power for the medium and water, respectively. Furthermore, for specified photon beam energy the same medium dependent conversion factor can be applied all through the treatment field since the stopping power ratio is independent of the position in the field (27).
An EGS4 pre-processor (PEGS4) is used before the simulation has begun, creating data sets containing physical properties of each material. Therefore, parameters such as mean free paths, scattering cross sections and electron stopping powers are possible to generate (26).

CERR®

Computational environment for radiotherapy research (CERR®) is written in the MATLAB© language and is used to import and display DICOM-RT format (25). When the DICOM dataset is imported into CERR® the whole plan archive is stored in a MATLAB© binary format. Subsequently, CERR provides a variety of possibilities such as DVHs and treatment planning comparisons (28; 29).

Materials and methods

Materials and methods used in this study are presented separately.

Patient material

RapidArc® beam delivery was performed using a Varian Clinac 2300 iX for nine clinical prostate treatment plans and one head and neck treatment plan with and without introduced errors (Table 1). All treatment plans had been created according to standard treatment planning routines at Herlev University hospital but not all had been used clinically.

Table 1. Specification of all treatment plans applied in the study.

Patient	Cancer site	Amount of MU	Energy [MV]	Total absorbed dose [Gy]
1	Prostate	483	15	70
2	Prostate	490	15	78
3	Prostate	399	15	78
4	Prostate	453	15	78
5	Prostate	434	15	78
6	Prostate	403	15	68
7	Prostate	421	15	68
8	Prostate	419	15	78
9	Prostate	431	15	78
10	H&N	314	6	66

Introduction of systematic errors

The DICOM plan files were exported from Eclipse™ v. 8.9 and systematic errors were introduced by shifting the position of the entire X1 MLC bank (Figure 3). Systematic errors introduced were ±0.5 mm, ±1.0 mm, ±1.5 mm and ±2.0 mm, thus a larger and smaller aperture was implemented simulating erroneous beam delivery, such as a calibration error. The minus and plus signs corresponds to the direction that results in larger and smaller aperture, respectively. Consequently, verification of the limitations of dosimetric measurements was also enabled. Introduction of systematic errors were carried out using a script written in MATLAB© v. 7.6.0. Subsequently, erroneous treatment plans were re-imported to Eclipse™ and calculated using AAA. Reference plans (i.e. with no introduced errors) were used to demonstrate the impact of the introduced errors.

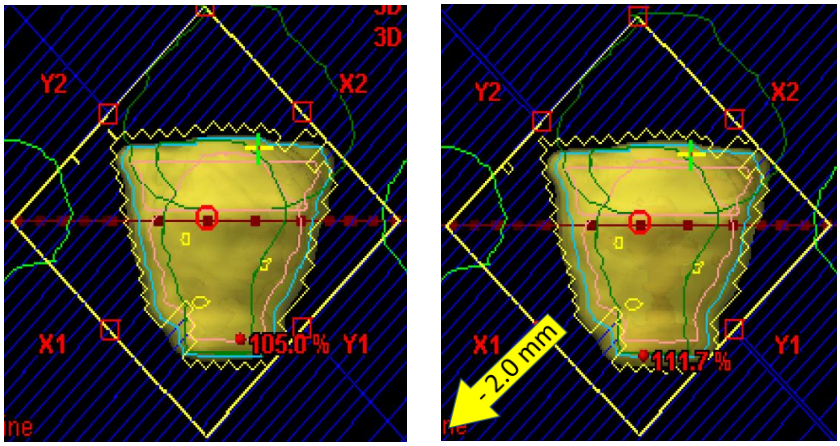

(a) Reference plan (b) The MLC bank shifted -2.0 mm

Figure 3. The position of the two MLC banks in the reference plan (a) and (b) erroneous plan with one of the MLC bank shifted -2.0 mm are displayed. The yellow arrow points out the direction shifting the entire MLC bank -2.0 mm thus larger separation between the two MLC banks occurred. In this particular case a larger aperture was enabled.

Dosimetric measurements

All dosimetric measurements were performed on the same Varian Clinac 2300 iX to reduce inter-accelerator uncertainties. Measurements were carried out using dosimetric equipment Delta$^{4®}$ (ScandiDos AB, Uppsala, Sweden) which is part of the standard RA QA system at Herlev University hospital. It consists of 1,069 disc shaped p-type Silicon diodes with a volume of 0.04 mm^3. The Delta$^{4®}$ equipment consists of two orthogonal diode arrays inside a cylindrical polymethylmethacrylate (PMMA) phantom, capable to measure the absorbed dose distribution in a 360° gantry rotation (Figure 4). The consecutive distance between diodes is 0.5 cm in the central area (6×6 cm^2) and 1.0 cm in the outer area (20×20 cm^2) of the planes. The phantom has a length of 40 cm and a diameter of 22 cm. The technical specifications for the ScandiDos Delta$^{4®}$ are listed in Appendix 3. For each measurement, the dosimetric system is able to divide absorbed dose information into sub beam structures related to the CP:s from the TPS. The RapidArc® treatment plans (RP and RD) were imported into the Delta$^{4®}$ software and therefore, information about the planned MLC and gantry positions were employed, allowing comparison between erroneous and reference treatment plans.

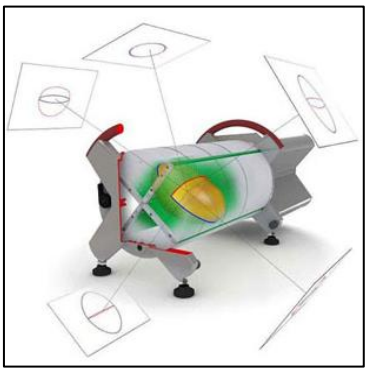

Figure 4. The Delta$^{4®}$ system

The gantry angle is measured using an inclinometer attached to the accelerator gantry and connected to the Delta$^{4®}$ system (Figure 5). Thus, the Delta$^{4®}$ system is able to identify which CP of the arc delivery that is being delivered and the measured absorbed dose is related to a specific CP. A RapidArc® plan is divided into 177 CP:s, categorizing MLC positions, cumulative MU between two CP and gantry angle. The absorbed dose of each CP contains the sum of dose pulses measured during the gantry angle interval of one CP. The equipment reports measured absorbed dose in relation to single accelerator pulses by applying a trigger signal

from the accelerator. Therefore, a time dependent four dimensional application is enabled.

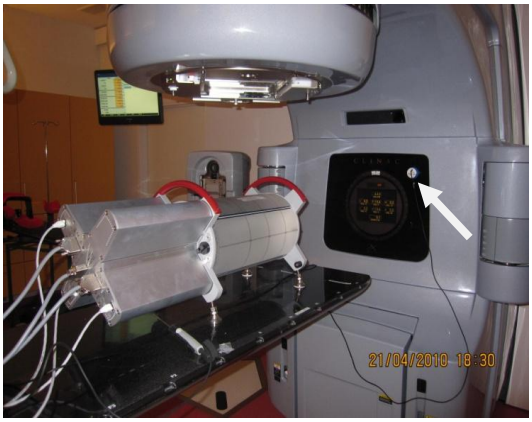

Figure 5. Dosimetric measurements were carried out with the Delta$^{4®}$ diode array, placed on the treatment couch. The white arrow points out the inclinometer connected to the gantry, which identifies which CP of the arc delivery that is being delivered and the measured absorbed dose is related to a specific CP.

To perform a calibration of the Delta$^{4®}$ diode array, the absorbed dose should be determined with an ionization chamber, preferably a farmer chamber, in an ionization chamber calibration slab. Subsequently, the ionization chamber calibration slab is substituted by the calibration phantom, with the Delta$^{4®}$ units inserted, at which a relative and an absolute calibration can be performed. It is recommended to perform both relative and absolute calibration at the same time (23). The relative calibration determines an individual relative sensitivity factor for every detector, which is used to compensate differences between detectors in the diode arrays.

The relative calibration is performed by irradiating the detector board consecutively in different positions inside a large field with a constant number of MU, therefore, all detectors are consecutively placed into positions where the absorbed dose is known.

After the irradiation is completed, for each detector position, the detector signals should be analyzed to check if there are any detectors that indicate a strong deviating signal. When the calibration is completed, the calibration factor-distribution should appear as a Gaussian distribution. Detectors with factors that fluctuates more than 30% of the average value should be further investigated (23).

When dosimetric measurements are carried out with the cylindrical Delta$^{4®}$ phantom, a 3D absorbed dose distribution is calculated. Since the planned absorbed dose is known in the entire cylindrical volume and the measured absorbed dose is known in the two orthogonal detector planes a calculation of the 3D absorbed dose distribution is possible. The 3D absorbed dose is calculated by means of renormalizing the planned absorbed depth dose along each beam ray using the ratio between the planned absorbed dose and the intersection position of the beam ray with the detector plane (Figure 6) (24).

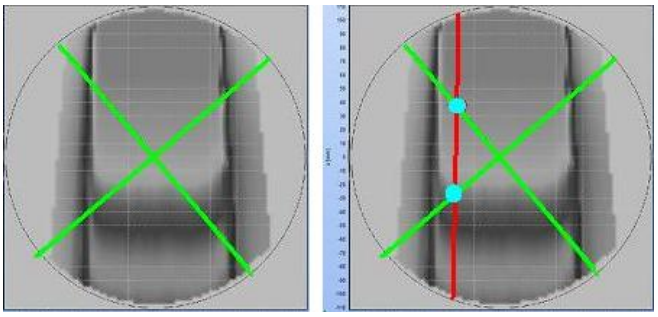

Figure 6. The image shows the variables used when the 3D absorbed dose distribution is calculated. The grey area is the planned absorbed dose, the green lines correspond to the two orthogonal detector planes, the blue dots represent the measured absorbed dose and the red line corresponds to the beam ray.

Furthermore, DVHs are calculated using several regions of interest (ROIs) inside the Delta$^{4®}$ phantom. These ROI are identical to the imported patient structures, from Eclipse™, in both position to the isocenter and shape (Figure 7). For each selected ROI the Delta$^{4®}$ software applies the planned and the measured 2D absorbed dose distributions to calculate the DVHs (24).

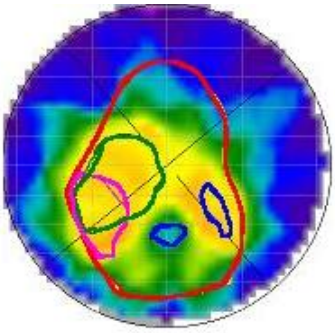

Figure 7. The defined ROIs correspond to the imported patient structure in both shape and position to the isocenter. These ROIs are used when DVHs are calculated.

Evaluation tools

The Delta$^{4®}$ software offers an evaluation tool where the patient´s structure is used to investigate whether deviations between measured and calculated absorbed dose deviations are of clinical importance. Thus, an evaluation whether, or not, deviating points are located inside critical structures is enabled. Furthermore, analysis of clinical relevance of a discrepancy in full 3D and dose comparison tools such as DVHs, absorbed dose deviations, DTA and gamma analysis (24) is possible. Since the gamma index distribution sometimes might be insufficient, these tools are intended for full analysis (24). Absorbed dose deviations may also be displayed as superimposed patient structures on the 3D data set (Figure 8).

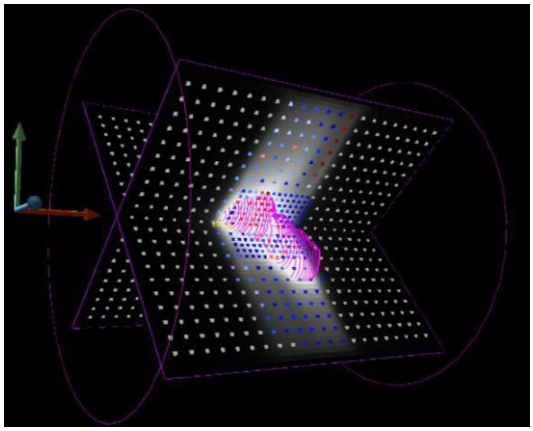

Figure 8. Superimposed patient structures on the measured 3D data set are applied when DVHs are created. The pink volume is the PTV.

RapidArc® absorbed dose calculations

The absorbed dose volume was calculated in Eclipse™ using the AAA with a grid size of 0.25 cm.

Evaluation methods

Absorbed dose distributions were evaluated using the gamma analysis as built into the Delta$^{4®}$ software. The acceptance criterion was set to 3% dose difference/3 mm DTA, which is in compliance with Korreman *et al* and Low *et al* (10; 22). The objective with the chosen acceptance criterion was to reflect a routine clinical condition. The Delta$^{4®}$ software displays the absorbed dose deviation from the planned absorbed dose, the DTA from the planned absorbed dose and the gamma index distribution, i.e. beam statistics, when treatment plans are to be evaluated (Figure 9). All three evaluation tools must be considered when evaluating absorbed dose distributions. Detectors included during measurements were in the dose range 20% to 500% of the maximum absorbed dose. The clinical impact of erroneous treatment plans was evaluated and comparison was carried out between:

- the fraction of passed gamma values for all measurements, the gamma index distribution, was defined to be when more than 90% of the data points had a gamma value ≤ 1 (Table 2)
- the percental planning target volume enclosed by $\geq$ 95% ($PTV_{95\%}$) of the prescribed absorbed dose [%]
- the volume enclosed by $\geq$ 95% and $\geq$ 105% of the prescribed absorbed dose ($V_{95\%}$, $V_{105\%}$) [cm^3]

Calculations of the $V_{95\%}$, $V_{105\%}$ were performed using a script written in MATLAB© and the values of the $PTV_{95\%}$ was obtained from Eclipse™. Furthermore, the change of the above defined volumes and with a passing rate of the gamma index above 90% was further investigated on a patient specific level.

Thus, cumulative DVHs was compared between

- reference- (i.e. without MLC offset) and erroneous treatment plans calculated with AAA.
- reference treatment plans calculated with AAA and measured data of erroneous treatment plans

Volumes studied using DVHs, were for the prostate patients, the PTV and rectum. For the H&N patient, the oPTV-T and medulla were chosen. The oPTV-T is the representing PTV-T used during the optimization process. The PTV-T defined by the physician is not applied in the optimization process because in some slices the volume is outside the body, i.e. in the air. Since the main objective was to investigate the impact of the introduced errors, only two volumes were selected for each treatment plan. Also, a qualitative evaluation of calculated reference and erroneous treatment plans were carried out in terms of percental absorbed dose difference with the objective to visualize the impact of introduced errors. The percental absorbed dose differences display spatial information of local dose discrepancies within the calculated volume dose. The percental absorbed dose difference was defined as:

$$D_{\%} = \frac{D_{Error} - D_{Ref}}{D_{Ref}} \times 100 \tag{9}$$

where D_{Error} and D_{Ref} is the absorbed dose of the erroneous and reference treatment plans, respectively. Furthermore, to visualize the volume change of $V_{95\%}$ the volume differences of reference and erroneous treatment plans were presented. Additionally, calculated reference plans and erroneous plans with a clinical impact were calculated by MC as an alternative QA protocol.

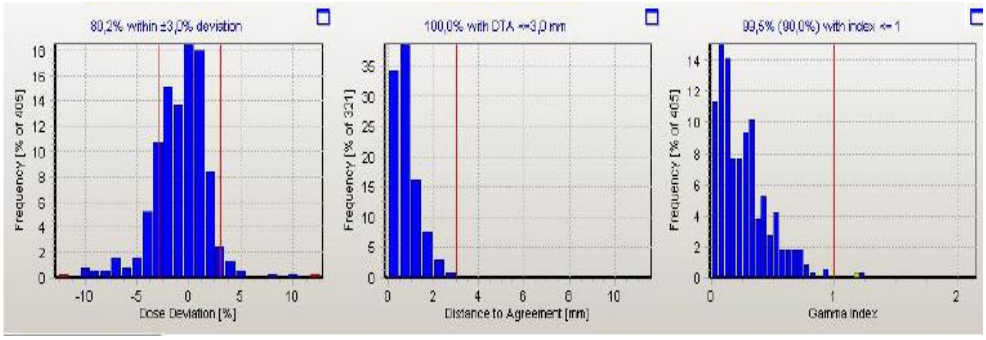

Figure 9. Beam statistics supplied by the Delta$^{4®}$ software. The left figure shows the absorbed dose deviation distributions from the planned absorbed dose, the centre figure shows the DTA from the planned absorbed dose and the right figure shows the gamma index distribution.

Monte Carlo model

MCSIM was used to simulate beam modifiers in the patient geometry such as blocks, jaws, and dynamic MLC fields (30) using a former simulation of the accelerator head named a phase space file (PSF) as a source input (26). The PSF was placed right below the flattening filter for all separate beam energies and was scored by simulation of approximately 2.5×10^6 histories. Cut off energies applied in the PSF were 521 keV and 10 keV for electrons and photons respectively (31). The PSF includes the type of particle, direction of motion, its position, statistical weight and energy for all particles reaching the PSF scoring plane. However, statistical weight is only required if variance reduction techniques is employed (32).

Variance reduction techniques are applied with the objective to reduce simulation time.

The treatment plan simulations were performed in MCSIM with only electron track repeating switched on as a variance reduction technique. Electron track repeating implies that the electron tracks are produced on the fly in a phantom with uniform density and tissue and can also be repeated in both tissue and other materials with variable densities (30; 31).

Monte Carlo absorbed dose calculations

Monte Carlo absorbed dose calculations were carried out as an alternative QA protocol for selected treatment plans of clinical importance, i.e. introduced errors not detected by using the Delta$^{4®}$ equipment (Figure 10). Introduced error of -1.0 mm for patient #4 was selected since this error was not explicitly detected by the Delta$^{4®}$ diode array. The objective was to demonstrate whether MC could detect absorbed dose differences by comparing DVHs between reference- and erroneous plans. A DICOM dataset was exported from Eclipse™ including computed tomography (CT) files, the plan file (RP) and the dose files (RD). The RP file was used to create an input file for MCSIM applying various scripts written in MATLAB©. Hence, all parameters of the treatment plans were recreated in the MC absorbed dose calculations. The input file contained:

- number of medium to be used
- gantry rotation
- geometry and simulation parameters
- source and beam setup parameters
- beam modifier description

Since the DICOM dataset are incompatible with MCSIM, the creation of a separate phantom file was required. An anthropomorphic phantom was built using DICOM-RT ctcreate as implemented in the DICOM-RT toolbox with the planning CT set as input (33; 34). Subsequently, MCSIM applies the created anthropomorphic phantom file, containing data of density distributions and materials, specified as input.

Reference and erroneous treatment plans were calculated with a simulation time of approximately 2 hours on one computer (Intel Core™2). The total number of histories was roughly 3×10^8 for each MC calculation and the uncertainty of the five highest dose areas was less than 1%. Calculations were carried out with a voxel size of $0.25 \times 0.25 \times 0.25$ cm^3. When the MC absorbed dose calculations were completed, a 3D absorbed dose output file was produced. This was converted into a DICOM format using CERR®. Thus, import to the TPS was enabled (Figure 9).

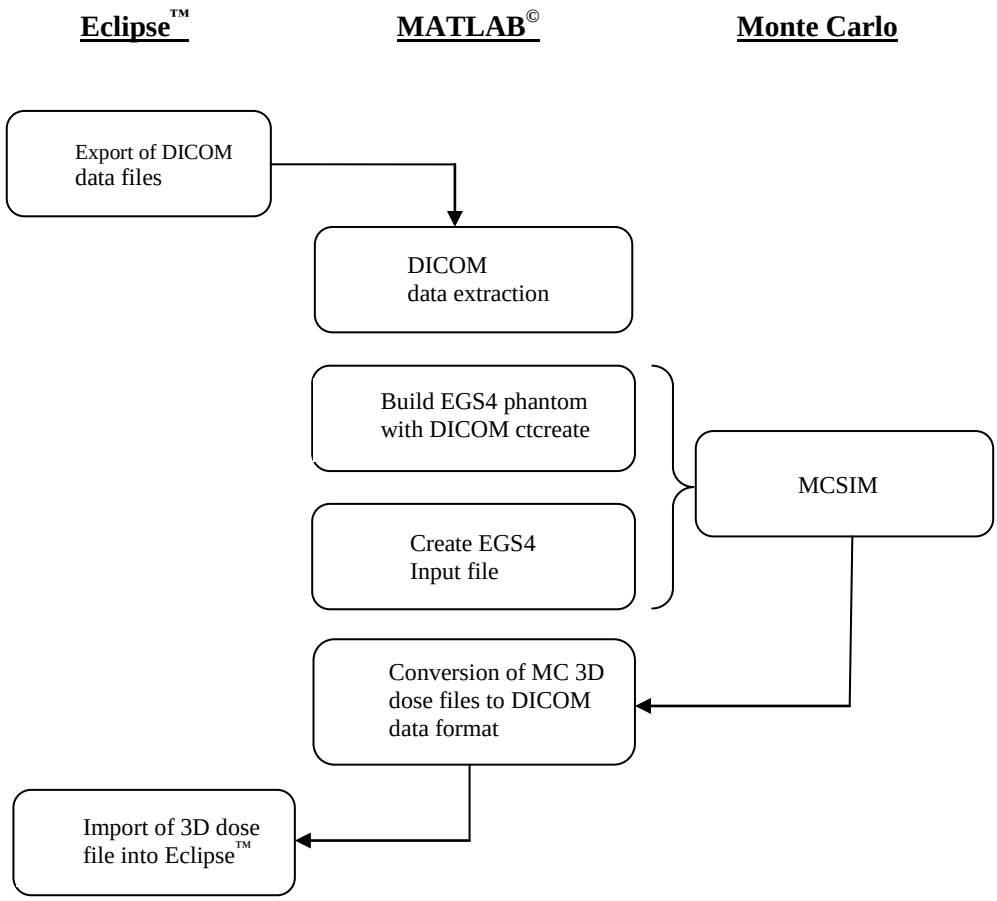

Figure 9. The scheme represents the workflow used when MC absorbed dose calculations were carried out as an alternative QA protocol.

CERR®

CERR® was used for import of 3D dose files created in MCSIM. The 3D dose files were imported into CERR® environment using a script written in MATLAB©, which converted 3D dose files into the MATLAB© binary format. Since MCSIM calculates dose to media and the TPS calculates dose to water, a conversion from MC calculated absorbed dose into absorbed dose to water was required to ensure correct dose comparison. The dose conversion method described by Siebers et al (27) as applied in the DICOM-RT toolbox (33) was utilized in CERR®. Additionally, CERR® environment was applied to convert the MATLAB© binary format to a DICOM format. Hence, import into Eclipse™ for absorbed dose comparison was made possible.

Results and discussion

The results from dosimetric measurements and calculated absorbed dose volumes were presented in a tabular form (Appendix 1). Treatment plans with introduced errors that passed the set gamma index evaluation criteria were further investigated on a patient specific level. The two different patient categories were presented separately. Various comparisons such as DVHs, calculated volumes were carried out between references, erroneous and measured absorbed dose distributions.

To visualize the clinical impact of introduced errors the percental absorbed dose differences and volume differences were reported. In compliance with the Delta$^{4®}$ system the absorbed dose deviation criteria was chosen to be ± 3%. The daily output between all measurements varied between - 0.09% and -0.4%.

Gamma analysis and calculated absorbed dose volumes

Maximum and minimum values of the fraction of passed gamma values (gamma index distribution) and calculated absorbed dose volumes were summarized for all introduced errors which were compared with reference plans, with the intention to visualize the extremes from measurements and calculated absorbed dose volumes (Table 2). Defined absorbed dose volumes indicate the clinical impact of introduced errors for prostate patients. For all introduced errors, percental change of $V_{95\%}$, and $PTV_{95\%}$ was reported. Furthermore, the increase of $V_{105\%}$ was presented in cm^3 since the $V_{105\%}$ was zero for almost every reference plan. Furthermore, these results disclose that a systematic error $\geq \pm$ 1.0 mm is a general limit which is detectable with the Delta$^{4®}$ diode array. If 3%/3mm DTA is applied, the acceptance criteria (i.e. the accepted fraction of passed gamma values) should be set to 95% instead of 90%, since this will reduce the risk of starting a clinically not accepted treatment plan. With the Delta$^{4®}$ diode array, systematic errors < +1.0 mm and $\leq$ -1.0 mm for prostate patients are in general not detected. The MLC bank shifted +1.0 mm resulted in a maximum and minimum decrease of the $PTV_{95\%}$ of 7.1% and 0.4% respectively, hence, not all errors were of clinical importance. With the MLC bank shifted -1.0 mm, the maximum and minimum increase of the $V_{95\%}$ was 20.3% and 7.4%, respectively. In general, an under dosage to the PTV in the original treatment plan, could benefit a small increase of the $V_{95\%}$, However, no under dosage of the PTV was seen for the studied treatment plans.

Introduced errors $\geq \pm$1.0 mm between MLC banks demonstrated an absorbed dose deviation distribution less than 70% within ± 3%. In some cases the absorbed dose deviation distributions within 3% were less than 50%. Thus, when evaluating absorbed dose distributions the absorbed dose deviation distribution is important to consider. If the absorbed dose deviation histogram is approximately a Gaussian distribution, with a standard deviation of 3.5%, about 85% of data points should be within 5% of the required value. The standard deviation should be set with respect to the prescription value and the required value should be normalized to the prescription absorbed dose (12). If a considerably number of data points fails to meet the absorbed dose agreement or the DTA, an investigation is necessary.

Moreover, not all introduced errors $\geq$ +1.0 mm and > -1.0 mm for prostate patients were detected using the gamma index distribution exclusively, but by means of the absorbed dose deviation tool all errors were detected. Thus, it is of great importance to use all evaluation tools such as the absorbed dose deviation, the DTA and the gamma index distribution when evaluating patient specific QA. Results from the H&N patient were also presented in tabular form (Table 5).

Table 2. Maximum and minimum values are displayed for dosimetric measurements and calculated absorbed dose volumes for prostate patients. Defined absorbed dose volumes show the impact of introduced errors for prostate patients. For all introduced errors, percental change of $V_{95\%}$ and $PTV_{95\%}$ is reported. The increase of $V_{105\%}$ is presented in cm^3.

MLC-bank [mm]	Gamma index [%]		$PTV_{95\%}$ [%]		$V_{95\%}$ [%]		$V_{105\%}$ [cm^3]	
	Min	Max	Min	Max	Min	Max	Min	Max
-0.5	95.1	100	100	100	104.5	113.3	0.5	3.6
-1.0	87.3	98.5	100	100	107.4	120.3	3.3	9.9
-1.5	75.3	92.4	100	100	110.2	126.2	7.7	25.7
-2.0	63.1	82.2	100	100	113.2	132.0	15.4	54.8
0	99.6	100	100	100	100	100	0	0.5
0.5	99.2	100	97.3	100	96.0	99.7	0	0
1.0	94.5	100	92.9	99.6	88.9	97.6	0	0
1.5	89.9	99.2	82.7	99.2	79.1	91.2	0	0
2.0	66.9	96.7	67.8	97.0	62.2	85.8	0	0

Patient specific evaluation

All patients were investigated on patient specific level (Appendix 1) but two prostate patients (patient #4 and patient #5) and one H&N patient (patient #10) are presented and discussed in this section due to their suitability in terms of clinical impact and on account of the results from dosimetric measurements.

Not all errors were detected using gamma index distribution evaluation solely, thus the beam statistics in the Delta$^{4®}$ software were also investigated. Normally, there is no defined absorbed dose deviation criterion as for the gamma index distribution; hence the appearance of the absorbed dose deviation distribution was contemplated. In terms of the DTA it was not possible to detect any of the introduced errors. Colourwash of absorbed dose distributions, topographical maps with 2D spatial information and the DVHs is displayed for the investigated erroneous treatment plans. Furthermore, the DVHs obtained from the Delta$^{4®}$ diode array should only be used as a qualitative supplement to the beam statistics due to small number of calculation points and subsequent uncertainties.

Patient #4

For this particular patient, introduced errors of +1.0 mm and -1.0 mm were chosen. The introduced error of +1.0 mm was selected to demonstrate the skewness of the absorbed dose distribution which is representative for all patients and clearly detected. Since the criterion of passed gamma values was satisfied and an under dosage of the PTV and an increase of the $V_{95\%}$ and $V_{105\%}$ occurred, these errors were considered clinically relevant. Other introduced errors for this patient were well detected by the dosimetric equipment or the clinical impact was negligible.

Gamma evaluation and calculated absorbed dose volumes

The systematic error of +1.0 mm showed a decrease of the $V_{95\%}$ by 10.5% compared to the reference plan (Table 3). Since the volume of the $V_{95\%}$ for this particular error was larger than the volume of the PTV the clinical impact was considered not relevant. However, the $PTV_{95\%}$ showed a decrease by 3.1% which was consid-

ered a clinically relevant deviation due to introduction of cold spots in the PTV. There was no increase of the $V_{105\%}$. This systematic error of +1.0 mm resulted in a fraction of passed gamma values of 94.5%.

The introduced systematic error of -1.0 mm showed an increase of the $V_{95\%}$ by 11.9% (from 192.5 cm^3 to 215.5 cm^3) compared to the reference plan (Table 3). This volume increase of the $V_{95\%}$ for this particular error was most definitely clinically relevant due to possible injuries of normal tissues. Moreover, there was an increase of the $V_{105\%}$ from 0.4 cm^3 to 9.9 cm^3. This was considered clinically relevant since the increase of $V_{105\%}$ indicates an introduction of hot spots. This systematic error of -1.0 mm resulted in a fraction of passed gamma values of 95.9%.

The introduced systematic error of +1.0 mm was not detected using gamma index evaluation solely. However, using the beam statistics available in the Delta$^{4®}$ software, a drastically skewed absorbed dose deviation distribution could be seen, where only 54.7% are within the ± 3% absorbed dose deviation criteria (Figure 10a). In the reference plan (Figure 10c) 78.2% are within the dose deviation criteria. This erroneous treatment plan is clearly not clinically acceptable and was well detected with the Delta$^{4®}$ diode array.

The introduced systematic error of -1.0 mm was not detected just by evaluating the result from the gamma index distribution. The beam statistics showed only a minor skewed absorbed dose deviation distribution where 75.9% are within the ± 3% absorbed dose deviation criteria (Figure 10b). Compared with reference plan (Figure 10c) it is not evident that one would detect this type of error. Therefore, it is important to accurately investigate the absorbed dose deviation distribution. This erroneous treatment plan was not obviously detected with the Delta$^{4®}$ diode array

Table 3. Results from dosimetrically measured and calculated absorbed dose volumes are presented. Displayed introduced errors of clinical importance produced with accepted gamma index.

MLC bank [mm]	Gamma index [%]	$V_{95\%}$ [%]	$PTV_{95\%}$ [%]	$V_{105\%}$ [cm^3]
-0.5	98.3	107.1	100.0	2.8
-1.0	95.9	111.9	100.0	9.9
-1.5	87.2	117.1	100.0	25.7
-2.0	78.6	122.1	100.0	54.8
0.0	100.0	100.0	100.0	0.0
0.5	99.2	96.3	99.2	0.0
1.0	94.5	89.5	96.9	0.0
1.5	89.9	79.1	88.9	0.0
2.0	83.2	62.9	71.5	0.0

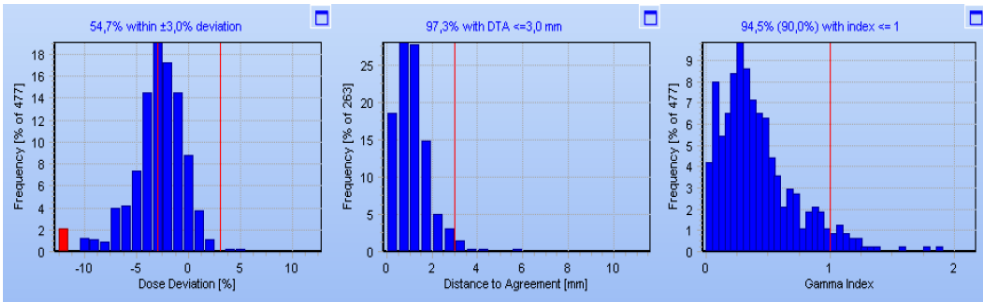

(a) The MLC bank shifted +1.0 mm.

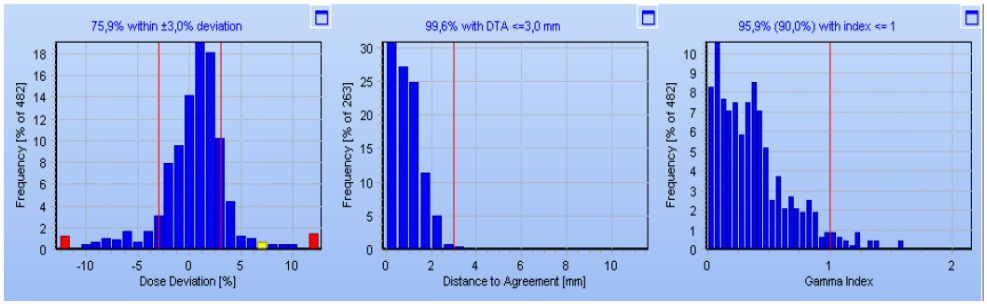

(b) The MLC bank shifted -1.0 mm

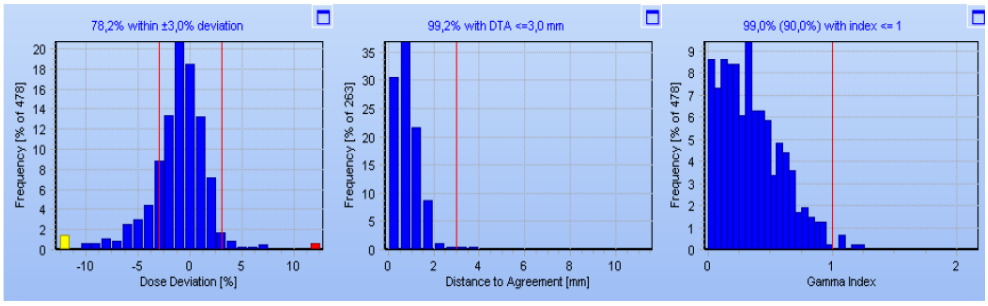

(c) Reference plan

Figure 10. Beam statistics obtained from the Delta$^{4®}$ software for the absorbed dose plan with (a) the MLC bank shifted +1.0 mm (b) the MLC bank shifted -1.0 mm and (c) the reference plan.

Evaluation of clinically important errors

A comparison was carried out between absorbed dose distributions in colourwash for reference plan and all erroneous plans (Figure 11a,b). Also, the percental absorbed dose was used for comparison.

The percental absorbed dose difference comparison between the reference plan and the MLC bank shifted -1.0 mm showed absorbed dose deviations larger than 3% mostly in the low dose regions but small absorbed dose deviations could be seen in the target region (Figure 11c) as implied in table 3. The percental absorbed dose difference of $V_{95\%}$ showed small deviations larger than 3% in the target region (Figure 11d). The increase of $V_{95\%}$ implies that a higher absorbed dose to the target region would have occurred with this erroneous treatment plan.

The percental absorbed dose difference comparison between the reference plan and the MLC bank shifted +1.0 mm demonstrated absorbed dose deviations larger than 3% mostly in the low dose regions but absorbed dose deviations could be seen in the target region (Figure 12c). The percental absorbed dose difference of $V_{95\%}$

shows small deviations larger than 3% in the target region (Figure 12d). Due to the decrease of $V_{95\%}$ the result showed that a lower absorbed dose to the target region would have occurred with this erroneous treatment plan.

The $V_{95\%}$ of reference plan and the MLC bank shifted -1.0 mm was also visualized (Figure 13a,b). Due to difficulties to determine the difference between the two plans, the volume difference was also presented (Figure 13c). The volume increase of erroneous treatment plan was clearly demonstrated. This particular error was not detected by means of the absorbed dose deviation tool or the gamma evaluation.

Moreover, the $V_{95\%}$ of reference plan and the MLC bank shifted +1.0 mm was presented (Figure 14a,b). The decrease of the $V_{95\%}$ is shown, as well (Figure 14c). There was a clinically relevant decrease of the absorbed dose within the target region. This particular error was detected by means of the absorbed dose deviation tool.

To further investigate the clinical impact of the introduced errors and the sensitivity of the Delta$^{4®}$ diode array, the DVHs from both Eclipse™ and the Delta$^{4®}$ diode array were studied and compared (Figure 15 a,b,c,d). Concerning the Delta$^{4®}$ software, the systematic error of -1.0 mm was not possible to visualize by studying the DVHs since no differences can be seen (Figure 15a). However, the DVHs calculated in Eclipse™ demonstrates an over dosage to the PTV. Regarding the Delta$^{4®}$ software, the systematic error of +1.0 mm was detected by studying the DVHs, large differences between planned and measured results were visualized (Figure 15c). The DVHs obtained from Eclipse™ shows an under dosage of the PTV. This particular error was detected by the Delta$^{4®}$ diode array in terms of DVHs and the absorbed dose deviation tool supplied in the beam statistics.

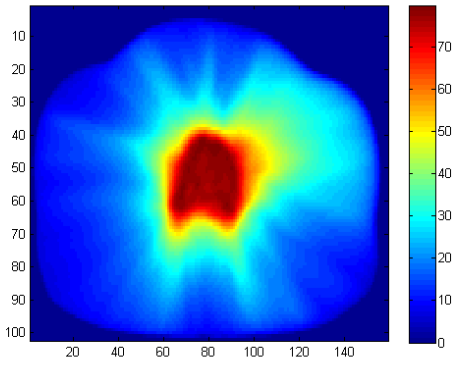

(a) Reference plan. The scale is in Gy.

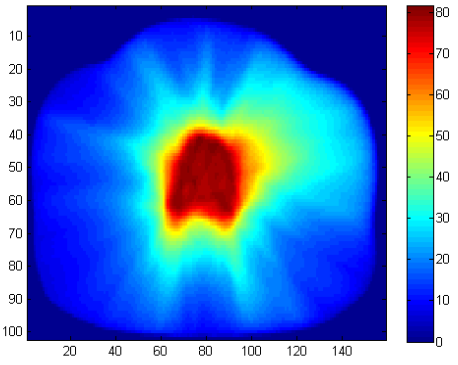

(b) The MLC bank shifted -1.0 mm. The scale is in Gy.

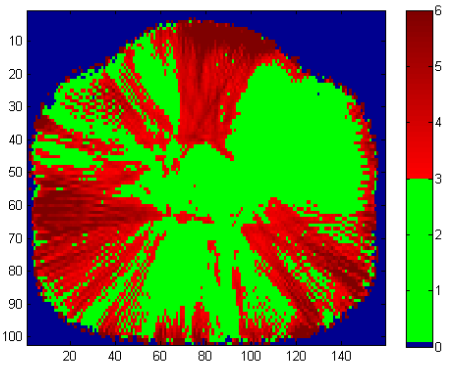

(c) Percental absorbed dose difference. The scale is in %.

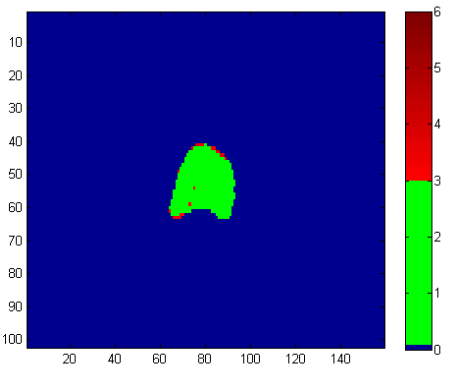

(d) Percental absorbed dose difference of $V_{95\%}$. The scale is in %.

Figure 11. Comparisons are carried out between the reference plan (a) and the plan with the introduced error, the MLC -1.0 mm, (b) absorbed dose distributions. Percental absorbed dose difference was investigated (c) as well as percental absorbed dose difference of $V_{95\%}$ (d).

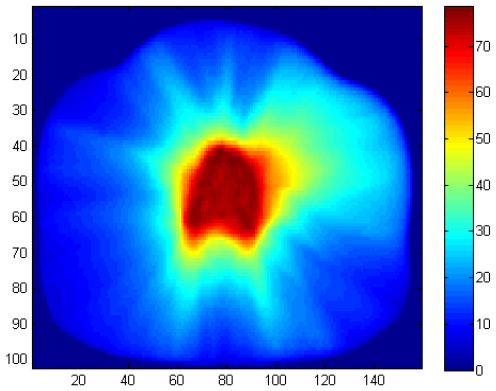

(a) Reference plan. The scale is in Gy.

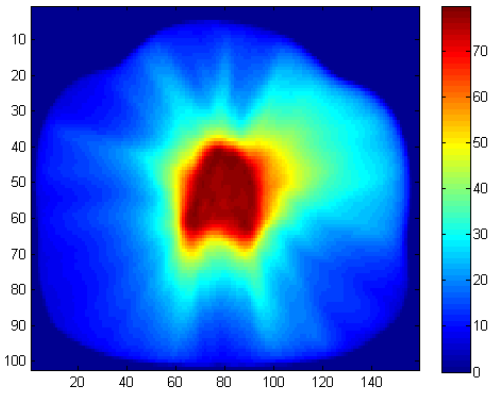

(b) The MLC bank shifted +1.0 mm. The scale is in Gy.

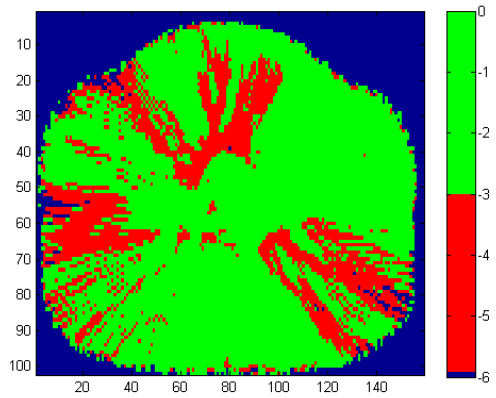

(c) Percental absorbed dose difference. The scale is in %.

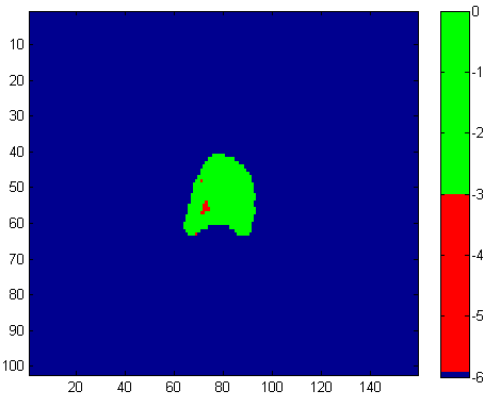

(d) Percental absorbed dose difference of the $V_{95\%}$. The scale is in %.

Figure 12. Comparisons are carried out between the reference plan (a) and the plan with the introduced error, the MLC +1.0 mm, (b) absorbed dose distributions. Percental absorbed dose difference was investigated (c) as well as percental absorbed dose difference of $V_{95\%}$ (d).

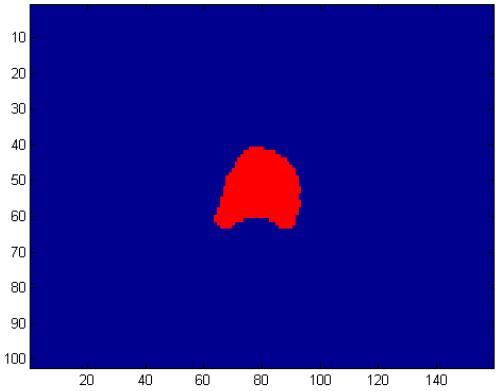

(a) Reference plan

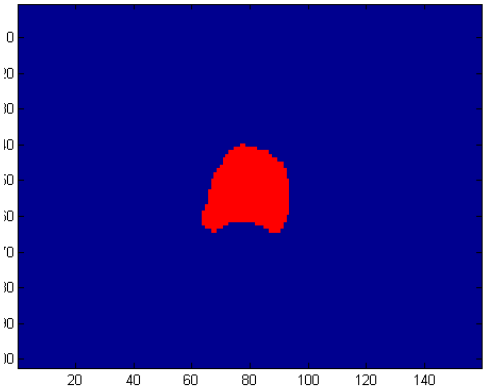

(b) The MLC bank shifted -1.0 mm

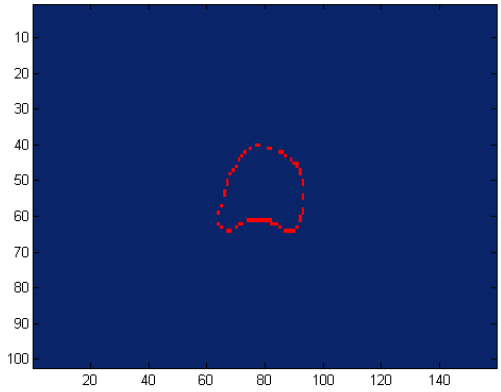

(c) The volume difference between reference plan and the MLC bank shifted -1.0 mm

Figure 13. Figures (a), (b) and (c) shows the volume in cm^3. Comparison between calculated $V_{95\%}$ of (a) reference plan and (b) the plan with MLC bank shifted -1.0 mm. The $V_{95\%}$ was increased with 11.9% and the $V_{105\%}$ was increased from 0 to 9.9 cm^3. The volume difference (c) between reference plan and the plan with the MLC bank shifted -1.0 mm is also displayed. This systematic error resulted in a fraction of passed gamma values of 95.9%.

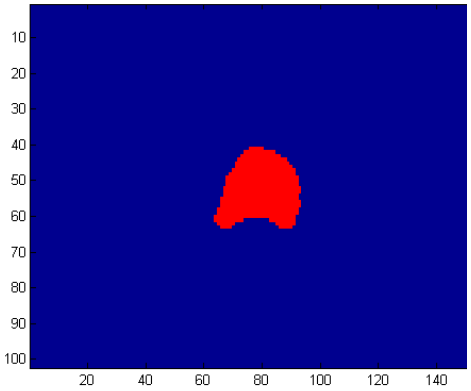

(a) Reference plan

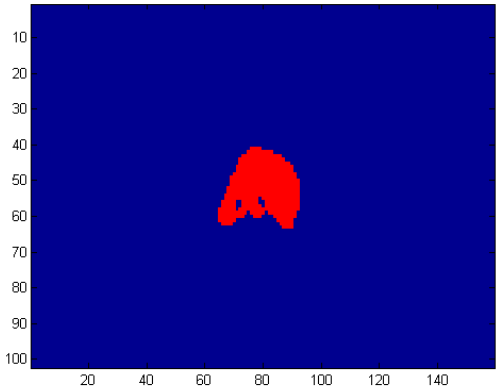

(b) The MLC bank shifted +1.0mm

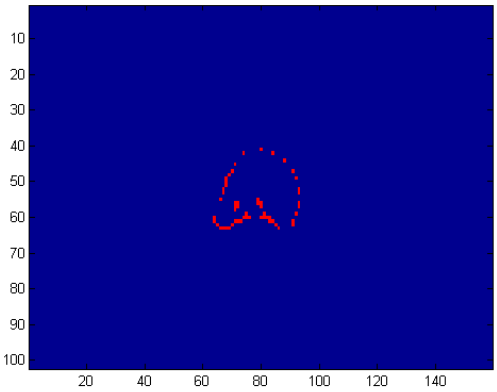

(c) The volume difference between the MLC bank shifted +1.0 mm and reference plan.

Figure 14. Figures (a), (b) and (c) shows the volume in cm^3. Comparison between calculated $V_{95\%}$ of (a) reference plan and (b) the plan with MLC bank shifted +1.0 mm. The $V_{95\%}$ was increased with 10.5% and the $PTV_{95\%}$ also decreased with 3.1%. The volume difference (c) between reference plan and the plan with the MLC bank shifted +1.0 mm is also displayed. This systematic error resulted in a fraction of passed gamma values of 95.9%.

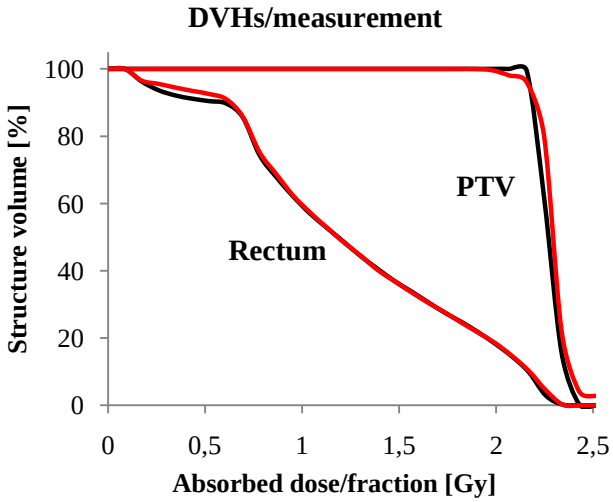

(a) Measured DVHs carried out with the Delta$^{4®}$ phantom. The red line is the MLC bank shifted -1.0 mm and the reference absorbed dose distribution is represented with the black line.

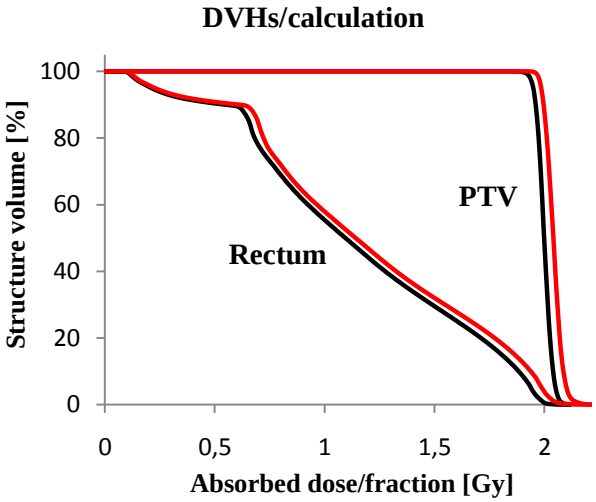

(b) DVHs calculated in Eclipse™ for the plan with the MLC bank shifted -1.0 mm (red line) and for the reference plan (black line).

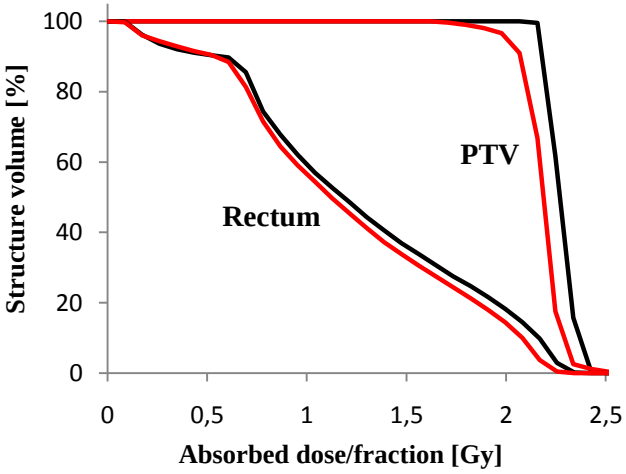

(c) DVHs from dosimetric measurements carried out with the Delta$^{4®}$ phantom. The red line represents the measured absorbed dose distribution when the MLC bank was shifted +1.0 mm and the reference absorbed dose distribution is represented with the black line.

.

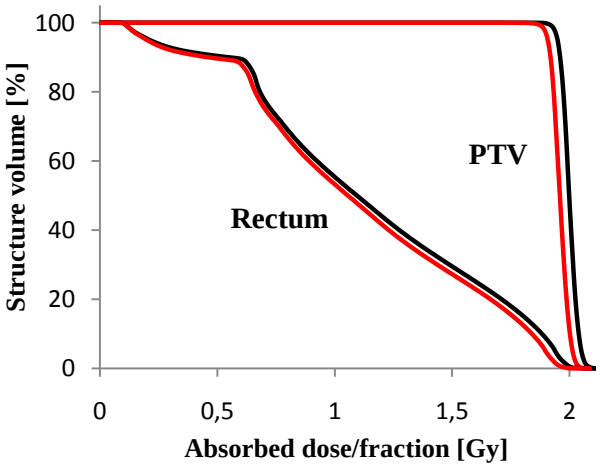

(d) DVHs calculated in Eclipse™ for the plan with the MLC bank shifted +1.0 mm (red line) and for the reference plan (black line).

Figure 15. The DVHs in (a) –and (c) is obtained from measured data with the MLC bank shifted -1.0 mm and +1.0 mm, respectively. The DVHs in the upper and lower right is calculated in Eclipse™ with the MLC bank shifted -1.0 mm and +1.0 mm, respectively.

Patient #5

For this particular patient, the absorbed dose plan with the introduced error of -1.0 mm was selected for visualization. This selection was done because, the erroneous absorbed dose distribution passed the gamma index evaluation, even though the $V_{95\%}$ and $V_{105\%}$ was increased to a clinically relevant level. Other introduced errors for this patient were well detected by the dosimetric equipment or the clinical impact was negligible.

Gamma evaluation and calculated absorbed dose volumes

The systematic error of -1.0 mm showed an increase of the $V_{95\%}$ by 12.3% (from 153.2 cm^3 to 172.1 cm^3) compared to the reference plan (Table 4). This volume increase of the $V_{95\%}$ for this particular error was most certainly clinically relevant due to possible injuries of normal tissues. There was also an increase of the $V_{105\%}$ from 0.0 cm^3 to 6.0 cm^3. This was clinically relevant, since the increase of $V_{105\%}$ indicates an introduction of hot spots. This systematic error of -1.0 mm resulted in a fraction of passed gamma values of 95.4%.

The introduced systematic error of -1.0 mm was not detected just by evaluating the result from the gamma index distribution. Also, the beam statistics demonstrated only a slightly skewed absorbed dose deviation distribution where 73.2% are within the ± 3% dose deviation criteria (Figure 16a). This erroneous treatment plan is clearly not acceptable and was not fully detected by the Delta$^{4®}$ diode array.

Table 4. Results from dosimetric measurements and calculated volumes are presented. Displayed introduced errors of clinical importance produced with accepted gamma index.

MLC bank [mm]	Gamma index [%]	$V_{95\%}$ [%]	$PTV_{95\%}$ [%]	$V_{105\%}$ [cm^3]
-0.5	99.5	107.4	100.0	1.4
-1.0	95.4	112.3	100.0	6.0
-1.5	85.0	116.1	100.0	15.1
-2.0	75.3	119.9	100.0	32.8
0.0	99.7	100.0	100.0	0.0
0.5	99.8	97.9	100	0.0
1.0	98.4	92.6	98.9	0.0
1.5	91.6	85.2	95.3	0.0
2.0	83.6	62.9	70.9	0.0

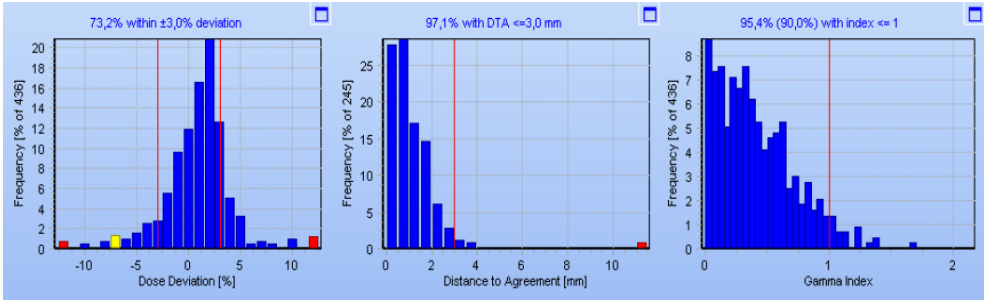

(b) The MLC bank shifted -1.0 mm

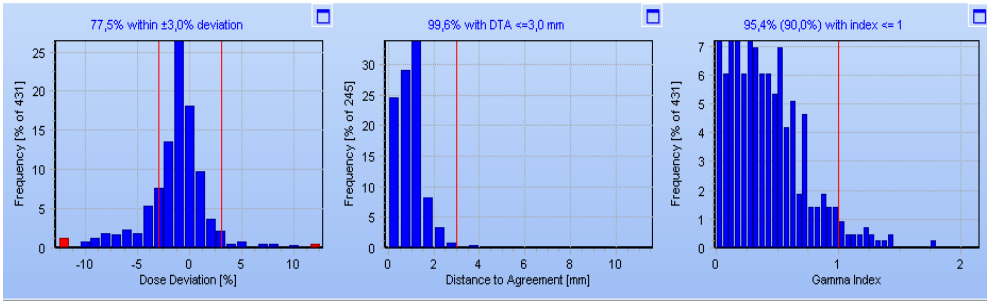

(c) Reference plan

Figure 16. Beam statistics obtained from the Delta$^{4®}$ software for (a) the MLC bank shifted -1.0 mm and (b) reference plan.

Evaluation of a clinically important error

The percental absorbed dose difference comparison between the reference plan and the plan with the MLC bank shifted -1.0 mm demonstrates small volumes of absorbed dose deviations larger than 3% in the target region. However, the absorbed dose deviations are mostly in the regions of low absorbed dose (Figure 17c). Only a small volume shows absorbed dose deviations larger than 3% in the target region according to the percental absorbed dose difference of $V_{95\%}$ (Figure 17d). A higher absorbed dose to the target region would have occurred with this erroneous treatment plan since the $V_{95\%}$ increased (Table 4).

The $V_{95\%}$ of reference plan and the MLC bank shifted -1.0 mm is also visualized (Figure 18a,b). The volume difference showing the volume increase of the erroneous treatment plan was presented (Figure 18c). Neither the absorbed dose deviation tool nor the gamma index distribution, demonstrated erroneous beam delivery.

The DVHs from both Eclipse™ and the Delta$^{4®}$ diode array were studied (Figure 19 a,b). Regarding the Delta$^{4®}$ software, the systematic error of -1.0 mm was not possible to detect by studying the DVHs, since no differences could be seen (Figure 19a). The DVHs calculated in Eclipse™ demonstrated an over dosage to the PTV which verifies the increase of the $V_{95\%}$, thus this error was considered clinically relevant. However, this particular error could not evidently be detected by the Delta$^{4®}$ diode array.

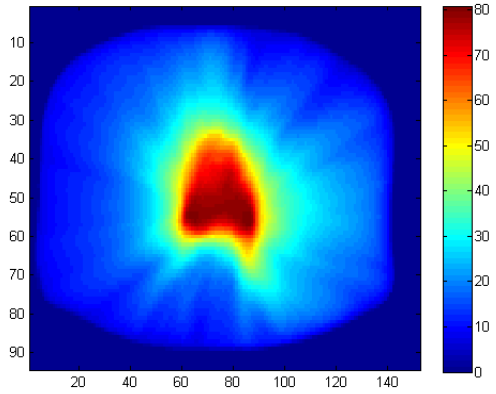

(a) Reference plan. The scale is in Gy.

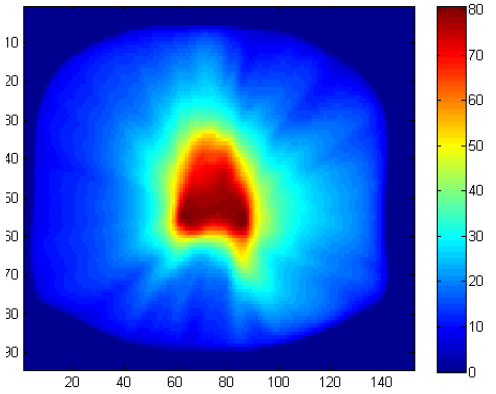

(b) The MLC bank shifted -1.0 mm. The scale is in Gy.

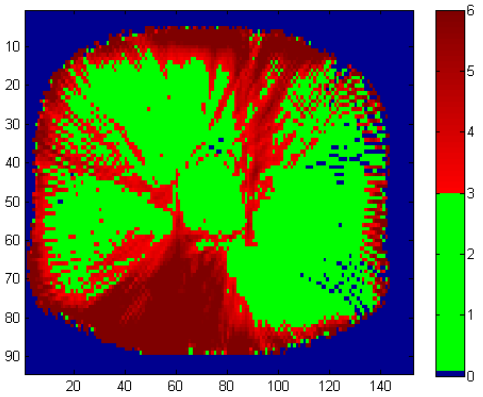

(c) Percental absorbed dose difference. The scale is in %.

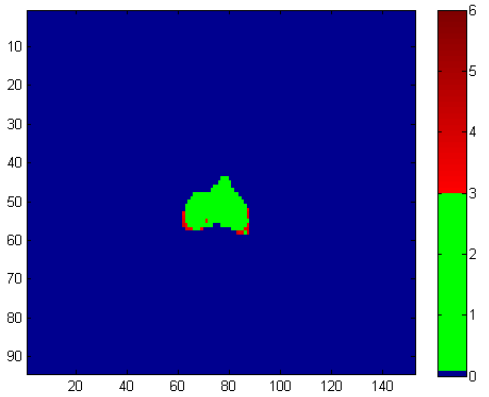

(d) Percental absorbed dose difference of $V_{95\%}$. The scale is in %.

Figure 17. Comparisons are carried out between the reference plan (a) and the plan with the introduced error, the MLC -1.0 mm, (b) absorbed dose distributions. Percental absorbed dose difference was investigated (c) as well as percental absorbed dose difference of $V_{95\%}$ (d).

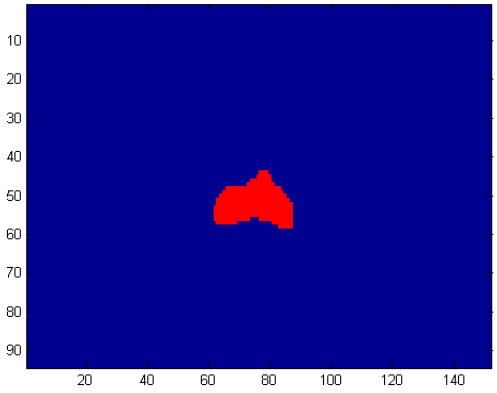

(a) Reference plan

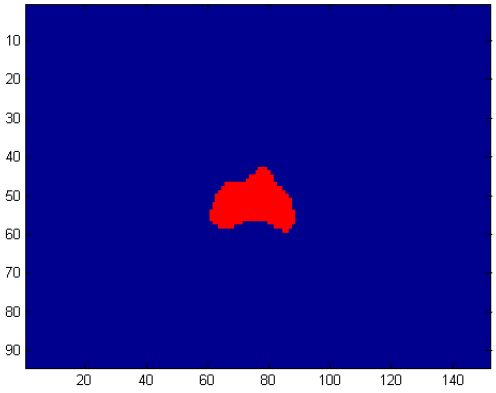

(b) The MLC bank shifted -1.0 mm

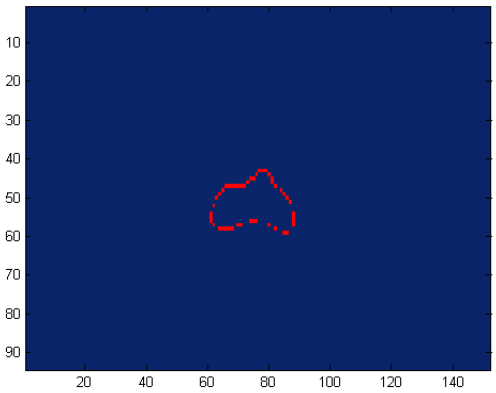

(c) The volume difference between reference plan and the MLC bank shifted -1.0 mm

Figure 18. Figures (a), (b) and (c) shows the volume in cm^3. Comparison between calculated $V_{95\%}$ of (a) reference plan and (b) the plan with MLC bank shifted +1.0 mm. The $V_{95\%}$ was increased with 12.3% and the $V_{105\%}$ increased from 0 to 6.0 cm^3. The volume difference (c) between reference plan and the plan with the MLC bank shifted -1.0 mm is also displayed. This systematic error resulted in a fraction of passed gamma values of 95.4%.

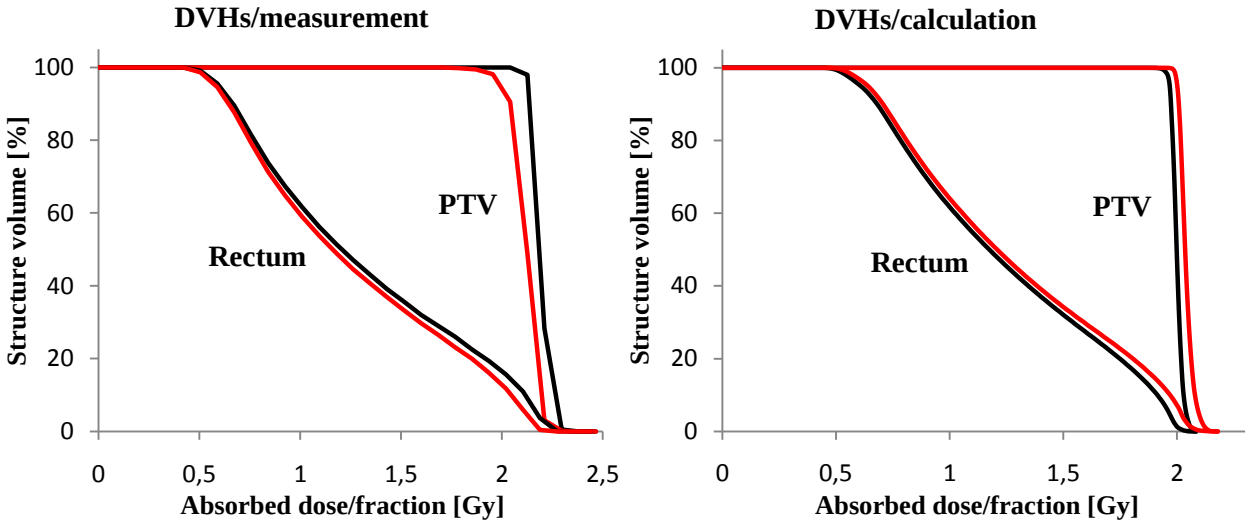

(a) Measured DVHs carried out with the Delta$^{4®}$ phantom. The red line is MLC bank shifted -1.0 mm and the reference absorbed dose distribution is represented with the black line.

(b) DVHs calculated in Eclipse™ for the plan with the MLC bank shifted -1.0 mm (red line) and for the reference plan (black line).

Figure 19. Comparison between measured and calculated DVHs for both PTV and rectum are displayed. The MLC bank was shifted -1.0 mm compared with the reference plan. The DVHs to the left is obtained from measurements with the MLC bank shifted -1.0 mm. The DVHs to the right is calculated in Eclipse™ with the MLC bank shifted -1.0 mm. This systematic error resulted in a fraction of passed gamma values of 95.4%.

Patient #10 (H&N)

For this patient, introduced error of -1.5 mm was selected. Since this error was clearly detected according to beam statistics in the Delta$^{4®}$ software and an increase of the $V_{95\%}$ eventuated, this error was considered clinically relevant.

Gamma evaluation and calculated dose volumes

The systematic error of -1.5 mm showed an increase of the $V_{95\%}$ by 5.7% (from 186.8 cm^3 to 197.7 cm^3) compared to the reference plan (Table 5). The increase of the $PTV_{95\%}$ was negligible. This volume increase of the $V_{95\%}$ for this particular error was of clinically importance due to irradiation of normal surrounding tissues and subsequent possible damage of normal tissues. There was no increase of the $V_{105\%}$ and this systematic error of -1.5 mm resulted in a fraction of passed gamma values of 98.9%. The introduced systematic error was not detected just by evaluating the result from measured data but the beam statistics demonstrated a slightly skewed absorbed dose deviation distribution where 73.6% are within the ± 3% absorbed dose deviation criteria (Figure 20a).

This erroneous treatment plan also showed a higher value in terms of passed gamma values compared to the reference plan. In this case it is quite important to thoroughly investigate the absorbed dose deviation distribution. The absorbed dose deviation tool is necessary to observe whether the absorbed dose distribution is skewed from the centre or not, since this indicates erroneous beam delivery. Studying the skewness of the absorbed dose deviation, combined with the percental absorbed dose deviation volume that are within the ± 3% absorbed dose deviation criteria is crucial. Introduced errors ≥ +1.0 mm for the H&N patient was not detected by using the gamma index distribution solely, but with the absorbed dose deviation tool these errors were detected. In this particular case, the plan with the MLC bank shifted -1.5 mm was not possible to detect by evaluating measured data.

Table 5. Results from dosimetric measurements and calculated volumes are presented. The results marked in red are further presented.

MLC bank [mm]	Gamma index [%]	$V_{95\%}$ [%]	$PTV_{95\%}$ [%]	$V_{105\%}$ [cm^3]
-0.5	97.8	102.3	99.3	0.0
-1.0	98.7	104.2	99.5	0.0
-1.5	98.9	105.7	99.6	0.0
-2.0	98.8	107.8	99,7	0.0
0.0	97.5	100.0	99.1	0.0
0.5	95.8	95.8	98.8	0.0
1.0	94.4	91.5	98.3	0.0
1.5	92.5	86.1	97.4	0.0
2.0	91.3	80.4	96.5	0.0

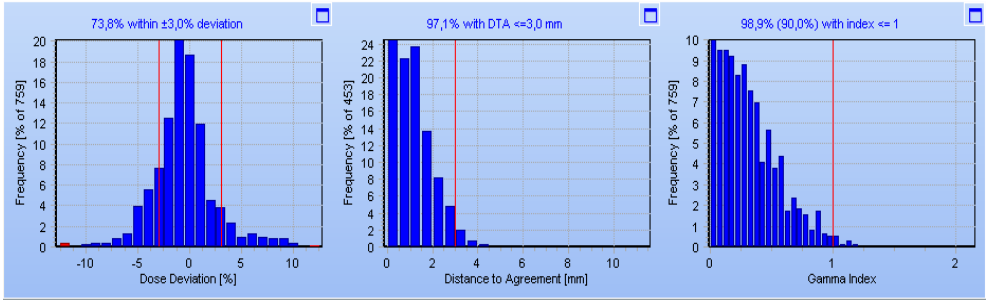

(a) The MLC bank shifted -1.5 mm

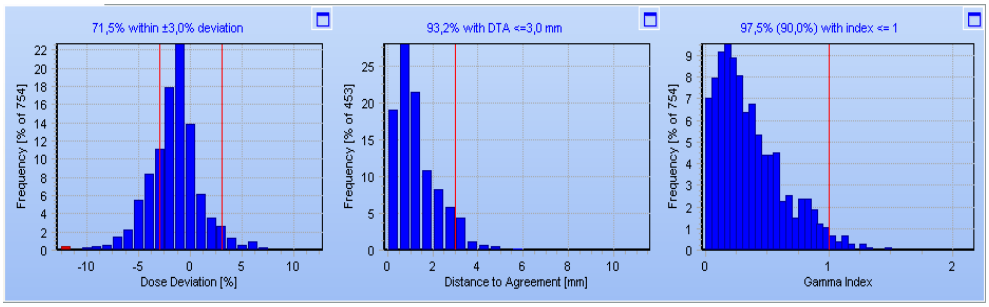

(b) Reference plan

Figure 20. Beam statistics obtained from the Delta$^{4®}$ software for (a) the MLC bank shifted -1.5 mm and (b) reference plan.

Evaluation of a clinically important error

The comparison of percental absorbed dose difference between the reference plan and the plan with the MLC bank shifted -1.5 mm demonstrated small volumes absorbed dose deviations larger than 3% in the target region. However, these absorbed dose deviations were mostly in the low dose regions (Figure 21c). Small deviations larger than 3% were shown in the target region according to the percental absorbed dose difference of $V_{95\%}$ (Figure 21d). A higher absorbed dose to the target region would have occurred with this erroneous treatment plan since the $V_{95\%}$ increased (Table 5).

The $V_{95\%}$ of reference plan and the plan with the MLC bank shifted -1.5 mm was also visualized (Figure 22 a,b). There was a volume increase of the $V_{95\%}$ for the erroneous treatment plan compared with the reference plan (Figure 22c). Compared with the treatment plans for the prostate patients, neither the absorbed dose deviation tool nor the gamma index distribution demonstrated erroneous beam delivery. However, there seemed to be a relevant clinical impact.

The DVHs from both Eclipse™ and the Delta$^{4®}$ phantom were studied (Figure 23a,b). The DVHs calculated in Eclipse™ demonstrates no visual difference and this particular error could not evidently be detected by the Delta$^{4®}$ diode array. The RA method is extraordinarily complex, and for complicated treatment plans such as H&N, the impacts of these types of introduced errors are not intuitively comprehensible.

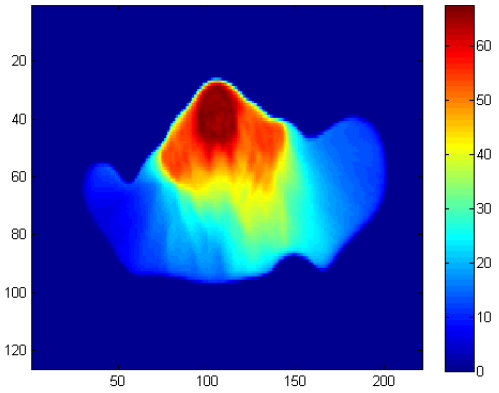

(a) Reference plan. The scale is in Gy.

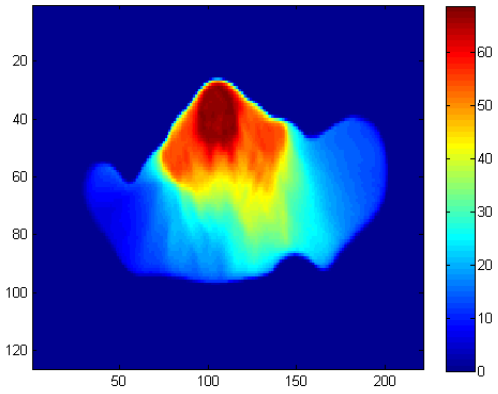

(b) The MLC bank shifted -1.5 mm. The scale is in Gy.

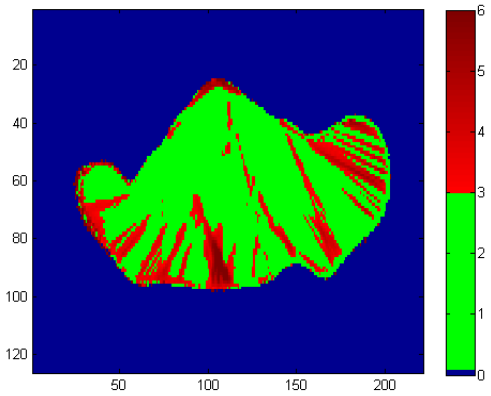

(c) Percental absorbed dose difference. The scale is in %.

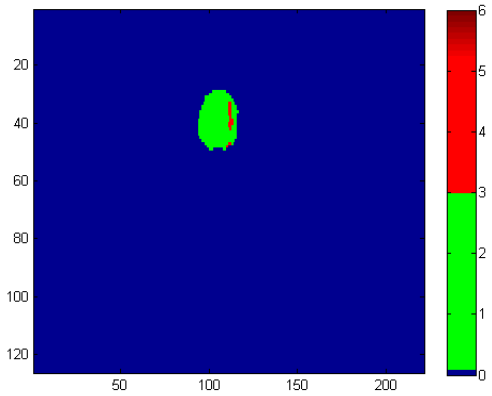

(d) Percental absorbed dose difference of $V_{95\%}$. The scale is in %.

Figure 21. Comparisons are carried out between the reference plan (a) and the plan with the introduced error, the MLC -1.5 mm, (b) absorbed dose distributions. Percental absorbed dose difference was investigated (c) as well as percental absorbed dose difference of $V_{95\%}$ (d).

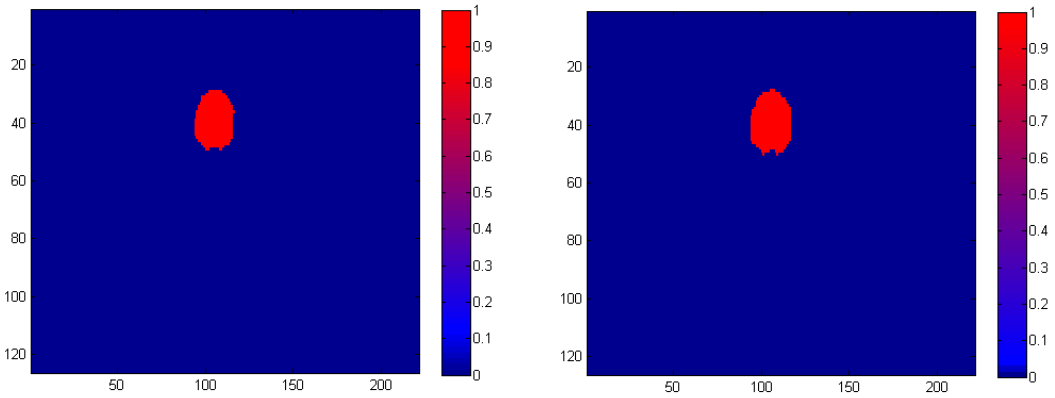

(a) Reference plan

(b) The MLC bank shifted -1.5mm

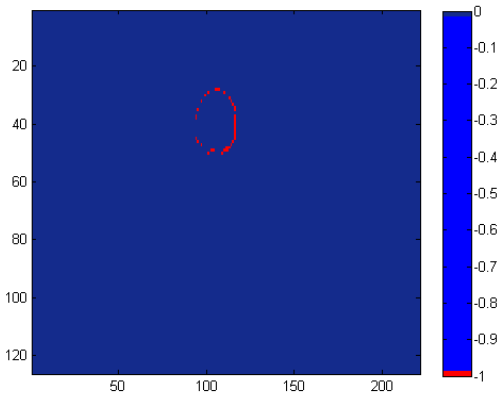

(c) The volume difference between reference plan and the MLC bank shifted -1.5 mm

Figure 22. Figures (a), (b) and (c) shows the volume in cm^3. Comparison between calculated $V_{95\%}$ of (a) reference plan and (b) the plan with the MLC bank shifted -1.5 mm. The $V_{95\%}$ was increased with 17.0%. The volume difference (c) between reference plan and the plan with the MLC bank shifted -1.5 mm is also displayed. This systematic error resulted in a fraction of passed gamma values of 98.9%.

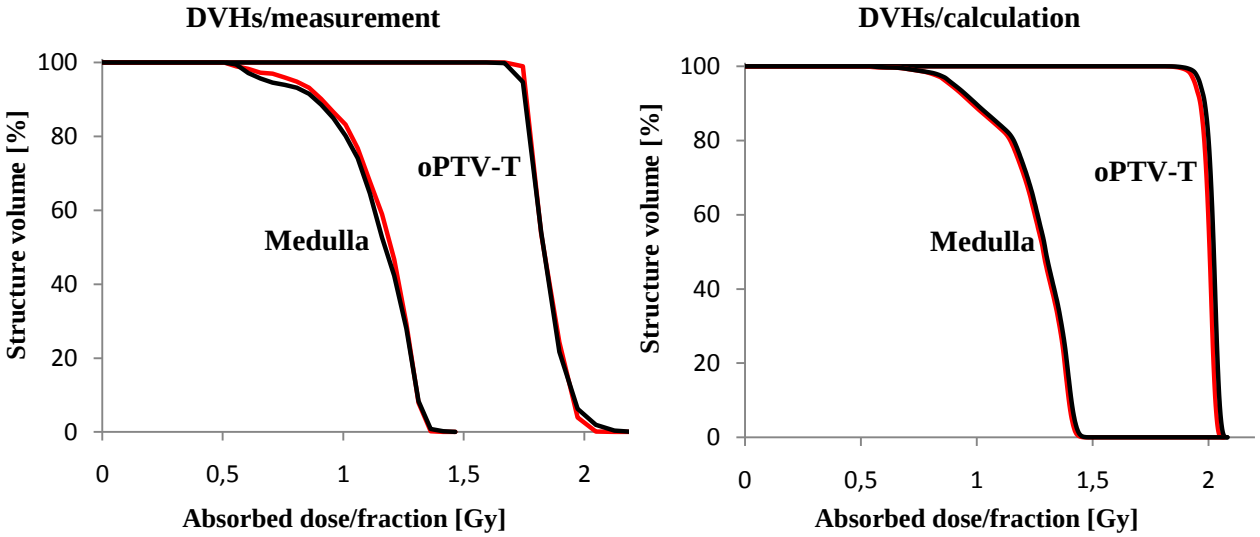

(a) DVHs from dosimetric measurements carried out with Delta$^{4®}$. The black line is MLC bank shifted -1.5 mm and the red line is reference plan.

(b) Calculated DVHs in Eclipse™. The black line is MLC bank shifted -1.5 mm and the red line is reference plan.

Figure 23. Comparison between measured and calculated DVHs for both oPTV-T and medulla are displayed. The MLC bank was shifted -1.5 mm compared with the reference plan. The DVHs to the right is obtained from measurements of erroneous beam delivery. The DVHs to the right is calculated in Eclipse™ with the MLC bank shifted -1.5 mm. This systematic error resulted in a fraction of passed gamma values of 98.9%.

MC absorbed dose calculations (Patient #4)

There were small percental absorbed dose deviations in the target region, which indicated a difference between treatment plans. (Figure 24c,d). Furthermore, the volume increase of the $V_{95\%}$ for the erroneous plan compared with the reference plan was evident (Figure 25a,b,c). The MC calculated DVH agrees well with the DVH calculated with AAA for prostate reference plans (Figure 25a). A comparison between the MC calculated DVH with the MLC bank shifted -2.0 mm and the DVH calculated with AAA, resulted in an over dosage to both the PTV and rectum (Figure 25b). Both the reference and the plan with the MLC bank shifted -1.0 mm and -2.0 mm was calculated with MC and the erroneous treatment plans was clearly visualized with the MC absorbed dose calculations (Figure 26 c,d).

When comparison was performed between reference plan calculated with the AAA and the plan with the MLC bank shifted -1.0 mm calculated with MC, there is an apparent difference (Figure 25c). The MC absorbed dose calculations could identify discrepancies between the reference and the selected erroneous treatment plans. This indicates that MC absorbed dose calculations can be a part of currently used QA in terms of quality control of TPS for comparison of different treatment plans.

However, problems with the machine QA cannot be discovered if the comparison of the TPS absorbed dose calculation is with MC absorbed dose calculation as an alternative of a measurement. It should be desirable to set an acceptance criteria, where MC could find potential TPS calculation errors hence MC could supplementing the Delta$^{4®}$ phantom for patient specific QA. Thus, a reduction of time consuming patient specific measurements could be achieved.

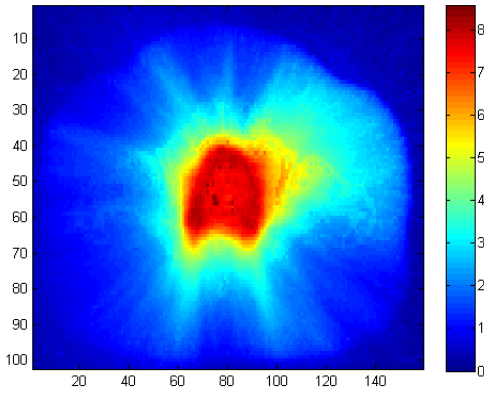

(a) Reference plan. The scale is in Gy

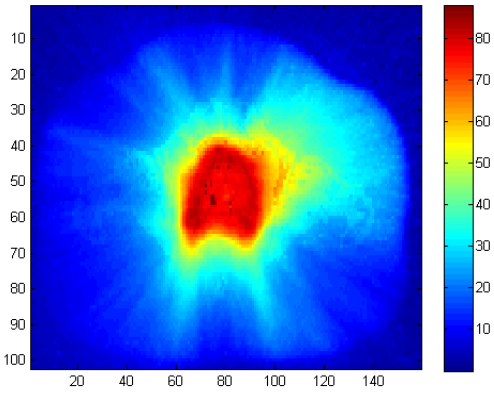

(b) The MLC bank shifted -1.0 mm. The scale is in Gy.

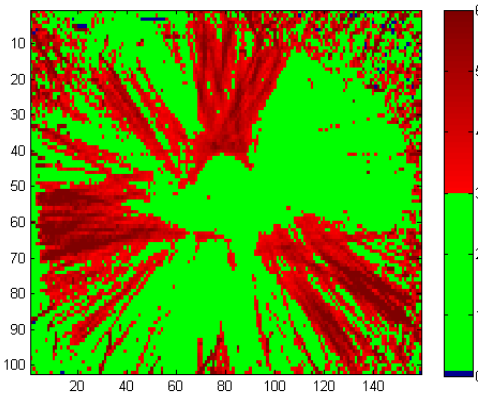

(c) Percental absorbed dose difference. The scale is in %

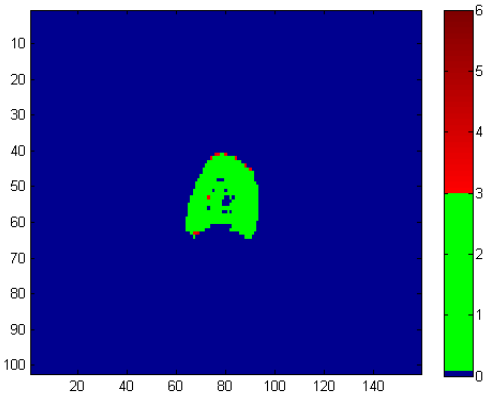

(d) Percental absorbed dose difference of $V_{95\%}$. The scale is in %

Figure 24. Colourwash between reference plan and MLC bank shifted -1.0 mm. Comparisons are carried out between (a, b) absorbed dose distribution, (c) percental absorbed dose difference and (d) percental dose difference of $V_{95\%}$.

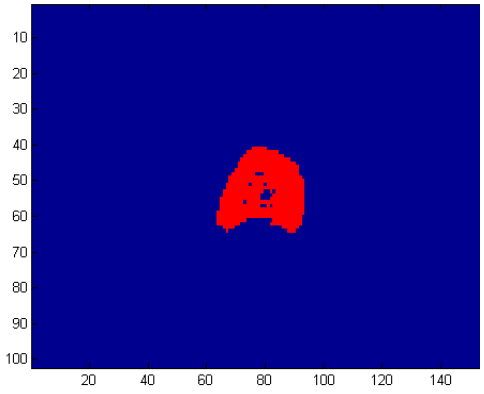

(a) Reference plan

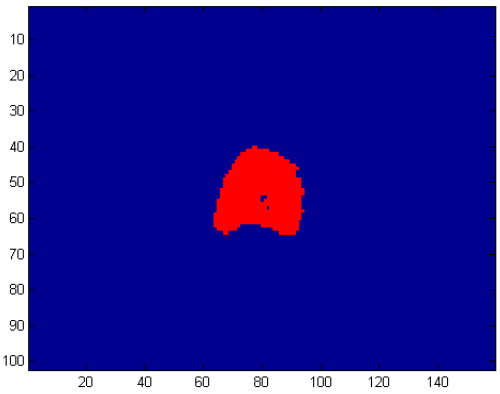

(b) The MLC bank shifted -1.0 mm

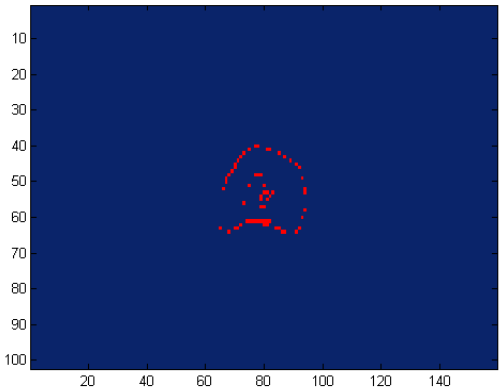

(c) The volume difference between reference plan and the MLC bank shifted -1.0 mm.

Figure 25. Figures (a), (b) and (c) shows the volume. Comparison between calculated $V_{95\%}$ of reference plan (a) and (b) the plan with the MLC bank shifted -1.0 mm.

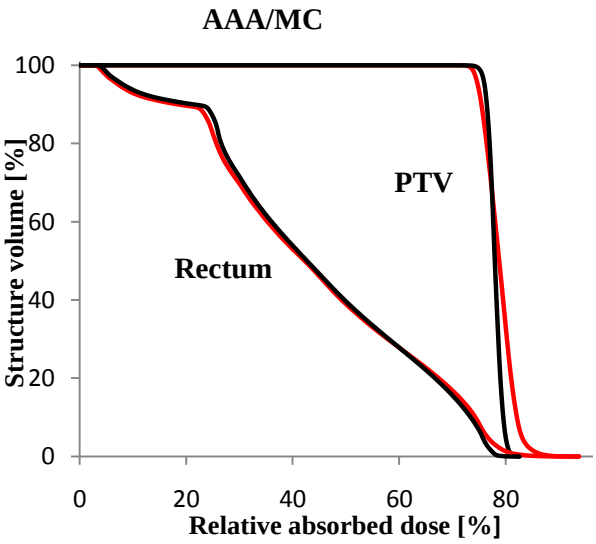

(a) Comparison between DVHs calculated with AAA (black line) and MC (red line). Calculations are performed for reference plans.

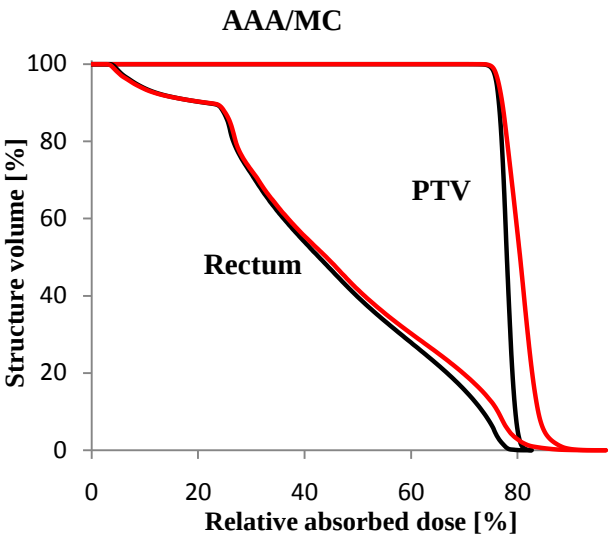

(b) Comparison between DVHs calculated with AAA (black line) and MC (red line). Calculations are performed for reference plans (AAA) and the MLC bank shifted -2.0 mm (MC).

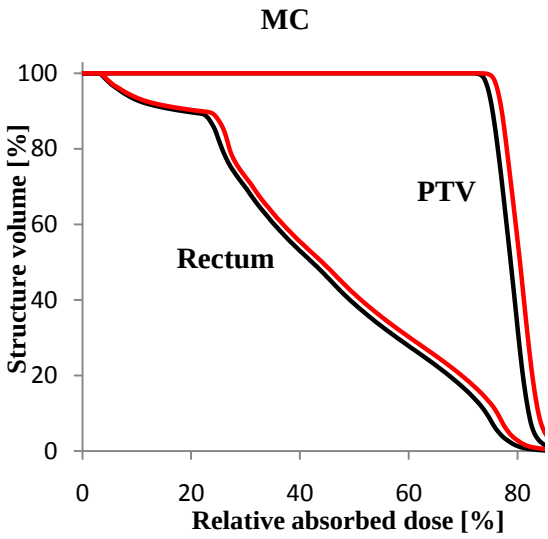

(c) Comparison between DVHs calculated with MC. The red line and black line corresponds to the MLC bank shifted -1.0 mm and the reference plan, respectively.

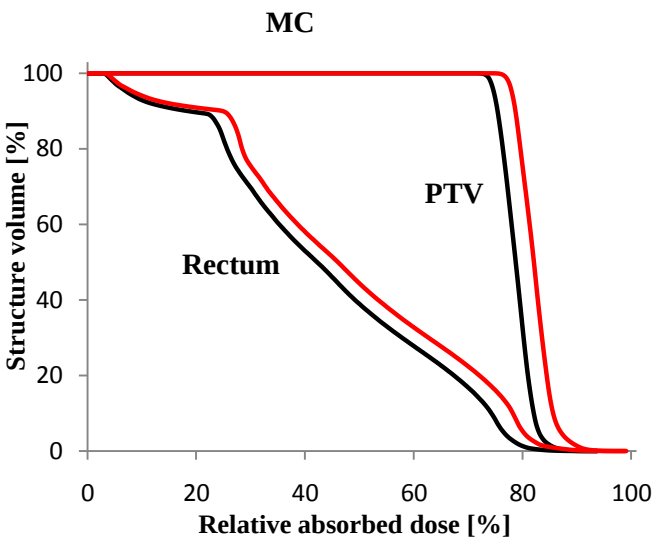

(d) Comparison between DVHs calculated with MC. The red line and black line corresponds to the MLC bank shifted -2.0 mm and the reference plan, respectively.

Figure 26. Comparison between AAA and MC for reference plan (a).The upper right DVHs is a comparison between reference plan and the MLC bank shifted -2.0 mm calculated with AAA and MC, respectively. The lower left DVHs is MC absorbed dose calculations for reference plan (black line) and the MLC bank shifted -1.0 mm (red line). The lower right DVHs is MC absorbed dose calculations for reference plan (black line) and the MLC bank shifted -2.0 mm (red line).

Conclusions

The impact of small changes in the position of the MLC bank might be of clinical importance and dosimetric measurements of introduced errors demonstrated that clinically important errors are not always detected with the currently used RA QA system for prostate treatment plans. Due to the complexity of the RA technique and various MLC movements between different treatments plans, the impact of shifting one of the entire MLC bank is very hard to anticipate. However, for prostate treatment plans, the results indicate that the Delta$^{4®}$ equipment is more sensitive when the aperture between the MLC banks is reduced. A further investigation is necessary for H&N treatment plans; however, for the investigated H&N treatment plan the indication was that the Delta$^{4®}$ equipment was more sensitive when the aperture between the MLC banks were reduced. Moreover, it is quite important to consider the beam statistics as built into the Delta$^{4®}$ software when performing patient specific RA QA.

Monte Carlo absorbed dose calculations are an excellent tool for visualizing differences between various treatment plans using DVHs. Therefore, MC absorbed dose calculations could complement, or replace, dosimetric measurements for patient specific RA QA. However, neither MC absorbed dose calculations using TPS generated plan files, nor the Delta$^{4®}$ diode array, can replace routine QA of the machine itself.

In the future, other introduced errors such as one stuck MLC leaf, incorrect beam energy and modified gantry rotation speed should be performed.

Bibliography

1. World Health Organization (WHO). *http://www.who.int/cancer/en/.* [Online]

2. Socialstyrelsen. *http://www.socialstyrelsen.se/Lists/Artikelkatalog/Attachments/17841/2009-12-1.pdf.* [Online]

3. Cancerfonden. *http://www.cancerfonden.se/Global/dokument/omcancer/cancer_i_siffror/Cancer_i_siffror_2009.pdf.* [Online]

4. U. Ringborg et al. *The Swedish Council on Technology Assessment in Health Care (SBU) Systematic Overview of Radiotherapy for Cancer including a Prospective Survey of Radiotherapy Practice in Sweden 2001 - Summary and Conclusions.* Acta Oncologica. 2003, Vol. 42, pp. 357–365.

5. Yu, Cedric X. *Intensity-modulated arc therapy with dynamic multileaf collimation: an alternative to tomotherapy.* Phys. Med. Biol. 1995, Vol. 40, pp. 1435-1449.

6. Otto, Karl. *Volumetric modulated arc therapy: IMRT in a single gantry arc.* Medical physics. 1, January 2008, Vol. 35, pp. 310-317.

7. Kjaer-Kristoffersen Flemming et al. *RapidArc volumetric modulated therapy planning for prostate cancer patients.* Acta Oncologica. 2008, Vol. 48, pp. 227-232.

8. Varian Medical Systems. *http://www.varian.com/.* [Online]

9. Gagne, I M et al. *A Monte Carlo evaluation of RapidArc dose calculations for oropharynx radiotherapy.* Phys. Med. Biol. 2008, Vol. 53, pp. 7167–7185.

10. Korreman Stine, Medin Joakim, Kjaer-Kristoffersen Flemming. *Dosimetric verification of RapidArc treatment delivery.* Acta Oncologica. 2009, Vol. 48, pp. 185-191.

11. Bush, K, Townson, R and Zavgorodni, S. *Monte Carlo simulation of RapidArc radiotherapy delivery.* Phys. Med. Biol. 2008, Vol. 53, pp. 359-370.

12. ICRU, International Commission on Radiation Units and Measurements. ICRU Report 83: *Prescribing, Recording, and Reporting Photon-Beam Intensity-Modulated Radiation Therapy (IMRT).* 2010.

13. Teke, Tony et al. *Monte Carlo based, patient-specific RapidArc QA using Linac log files.* Med. Phys. 2010, Vol. 37, pp. 116-123.

14. Schreibmann, Eduard et al. *Patient-specific quality assurance method for VMAT treatment delivery.* Med. Phys. 2009, Vol. 36, pp. 4530-4535.

15. Nicolini, Giorgiet et al. T*he GLAaS algorithm for portal dosimetry and quality assurance of RapidArc, an intensity modulated rotational therapy*. Radiat. Oncol. 2008, Vol. 3, pp. 24-34.

16. Bedford, J L, et al. *Evaluation of the Delta4 phantom for IMRT and VMAT verification.* Phys. Med. Biol. 2009, Vol. 54, pp. 167–176.

17. Rangel, Alejandra, Palte, Gesa and Dunscombe, Peter. *The sensitivity of patient specific IMRT QC to systematic MLC leaf bank offset errors.* Med. Phys. 2010, Vol. 37, pp. 3862-3867.

18. Fan, J, et al. *A practical Monte Carlo MU verification tool for IMRT quality assurance.* Phys. Med. Biol. 2006, Vol. 51, pp. 2503–2515.

19. Varian Medical Systems. *http://www.varian.com/us/oncology/treatments/treatment_techniques/rapidarc/.* [Online]

20. Fogliata, A, et al. *Dosimetric validation of the anisotropic analytical algorithm for photon dose calculation: fundamental characterization in water.* Phys. Med. Biol. 2006, Vol. 51, pp. 1421–1438.

21. Caprile, P, Venencia, C.D and Besa, P. *Comparison between measured and calculated dynamic wedge dose distributions using the anisotropic analytic*

algorithm and pencil-beam convolution. Journal of Applied Clinical Medical Physics. 2007, Vol. 8, pp. 47-54.

22. Low, Daniel A et al. *A technique for the quantitative evaluation of dose distributions.* Medical physics. May 1998, Vol. 25, pp. 656-661.

23. Delta4: Getting started. ScandiDos AB. Uppsala, Sweden : s.n., 2009.

24. ScandiDos AB. *http://www.scandidos.com/LinkClick.aspx?fileticket=AA6AN2hbT4w%3d&tabid=84&mid=504.* [Online]

25. Nelson, W.R and Namito, Yoshihito. *The EGS4 code system: Solution of gamma-ray and electron transport problems.* http://www.slac.stanford.edu/cgi-wrap/getdoc/slac-pub-5193.pdf. [Online] 1990.

26. Metcalfe, P, Kron, T and Hoban, P. *The Physics of Radiotherapy X-Rays and Electrons.* Madison: Medical Physics Publishing. 2007.

27. Siebers, J V, et al. *Converting absorbed dose to medium to absorbed dose to water for Monte Carlo based photon beam dose calculations.* Phys. Med. Biol. 2000, Vol. 45, pp. 983-995.

28. CERR. *http://radium.wustl.edu/CERR/about.php.* [Online]

29. Deasy, Joseph O., Blanco, Angel I. and Clark, Vanessa H. C*ERR: A computational environment for radiotherapy research.* Med. Phys. 2003, Vol. 30, pp. 979-985.

30. C-M Charlie Ma et al. MCSIM Users Manual. *MCSIM - A Monte Carlo Dose Calculation Tool for Radiation Therapy.*

31. Ottosson, R O, Karlsson, A and Behrens, C F. *Pareto front analysis of 6 and 15 MVdynamic IMRT for lung cancer using Pencil Beam, AAA and Monte Carlo.* Phys. Med. Biol. 2010, Vol. 55, pp. 4521-4533.

32. Sempau, J, et al. *Monte Carlo simulation of electron beams from an accelerator head using PENELOPE.* Phys. Med. Biol. 2001, Vol. 46, pp. 1163–1186.

33. Spezi, E, Lewis, D G and Smith, C W. *A DICOM-RT-based toolbox for the evaluation and verification of radiotherapy plans.* Phys.Med.Biol. 2002, Vol. 47, pp. 4223–4232.

34. Spezi, Emiliano. DICOM-RT Toolbox Manual.

Appendix 1

Displayed results are the fraction of passed gamma values obtained from measurements, performed by the Delta$^{4®}$ diode array.

MLC	Patient 1	Patient 2	Patient 3	Patient 4	Patient 5	Patient 6	Patient 7	Patient 8	Patient 9	Patient 10
-0,5	100	99,2	99,8	98,3	99,5	95,1	96,5	99,8	98,0	97,8
-1	97,5	93,5	98,5	95,9	95,4	87,3	89,3	97,6	89,6	98,7
-1,5	87,1	79,5	92,4	87,2	85,0	73,2	75,9	90,7	75,3	98,9
-2	75,3	68,3	82,2	78,6	71,3	64,5	63,1	78,3	65,2	98,8
0	100	99,5	100,0	100,0	100,0	100,0	100,0	100,0	100,0	97,5
0,5	100,0	100,0	100,0	99,2	99,8	100,0	99,6	99,8	100,0	95,8
1	98,9	99,8	99,1	94,5	98,4	99,5	99,1	99,2	99,3	94,4
1,5	93,4	80,0	96,1	89,9	91,6	96,6	99,2	98,5	95,1	92,5
2	93,4	93,3	96,4	83,2	83,6	94,5	96,7	96,0	66,9	91,3

Calculated volumes in cm^3 ($V_{95\%}$) for all treatment plans used in the study. Calculations were performed in the MATLAB© environment.

	Ref	**0.5**	**1.0**	**1.5**	**2.0**	**-0.5**	**-1.0**	**-1.5**	**-2.0**
Patient 1	75,0	71,3	70,4	68,4	65,	72,5	85,9	89,4	92,9
Patient 2	135,7	130,6	121,1	107,8	85,3	147,0	155,1	162,8	170,8
Patient 3	357,7	351,6	339,6	323,3	299,3	373,9	384,3	394,2	405,0
Patient 4	192,5	185,4	172,3	152,2	121,1	206,2	215,5	225,5	235,0
Patient 5	153,2	150,0	141,8	130,5	106,7	164,6	172,1	177,9	183,0
Patient 6	156,2	148,2	138,6	125,4	106,4	162,7	169,2	174,9	180,8
Patient 7	62,2	61,7	57,4	51,0	41,1	70,5	74,8	78,4	82,1
Patient 8	139,6	139,1	133,6	127,3	119,8	150,4	156,3	161,0	166,0
Patient 9	216,7	208,0	192,5	174,4	134,7	231,8	242,8	253,4	263,4
Patient 10	186,8	182,6	179,0	173,8	169,4	191,0	194,6	197,7	201,3

Appendix 2

Purpose: Currently, patient specific dosimetric measurements on diode arrays such as Delta$^{4®}$ (ScandiDos AB) is a part of standard quality assurance (QA) for RapidArc (RA). However, difficulties to interpret what results from dosimetric measurements represent in the patient geometry are a standing issue. Furthermore, measurements are time consuming. Thus, alternative QA systems are desirable for RA. The aims of this study were to investigate (1) the impact of introduced known errors, (2) whether clinically significant errors are detectable by current QA and (3) the benefits and drawbacks of dosimetric measurements and independent calculations for RA QA.

Materials and methods: Dynamic RA beam delivery was performed using a Varian Clinac 2300 iX for a number of clinical prostate plans with and without introduced errors. The DICOM plan files were edited and systematic errors were introduced by shifting the position of the MLC bank. Erroneous treatment plans were calculated in Eclipse using the analytic anisotropic algorithm (AAA) and were subsequently measured with Delta^4. The impact of erroneous treatment plans was evaluated in terms of clinical importance by comparison of the volume enclosed by ≥95% and ≥105% of the prescribed dose in the planning target volume ($V_{95\%}$, $V_{105\%}$). Delivered absorbed dose distributions were evaluated using gamma analysis as built into the Delta$^{4®}$ software with acceptance criteria set to 3% dose difference/3 mm distance-to-agreement. All treatment plans were calculated with Monte Carlo (MC) as an alternative QA protocol.

Results*:* A change in position of the MLC-bank ≥1 mm showed clinically relevant deviations according to over/under dosage in the PTV. Not all introduced errors of clinically significant deviations were detected with the dosimetric measurements hence acceptance criteria of the gamma factor were satisfied (Table). Also, the MC based QA protocol was able to detect the introduced errors.

Conclusions: Small changes in position of the MLC-bank are of clinical importance and dosimetric measurements of introduced errors demonstrated that clinically significant errors are not always detected with currently used RA QA. This study showed that small systematic errors could be detected with MC. Thus, MC might be used as a part of RA QA in the future.

Table . Comparison between min/max values of $V_{95\%}$, $V_{105\%}$ and gamma factor.

MLC-bank [mm]	$V_{95\%}$ [%]		$V_{105\%}$ [%]		Gamma factor [%]	
	Min	Max	Min	Max	Min	Max
0	99.4	99.8	0	0.2	99.3	100
0.5	99.0	99.2			99.2	100
1.0	96.0	97.8			94.5	99.8
1.5	88.9	95.4			80.0	96.1
2.0	71.5	89.9			83.2	96.4
-0.5			0.5	1.3	99.4	100
-1.0			1.6	6.4	95.9	98.5
-1.5			4.1	16.3	79.5	92.4
-2.0			8.1	37.6	68.3	82.2

Appendix 3

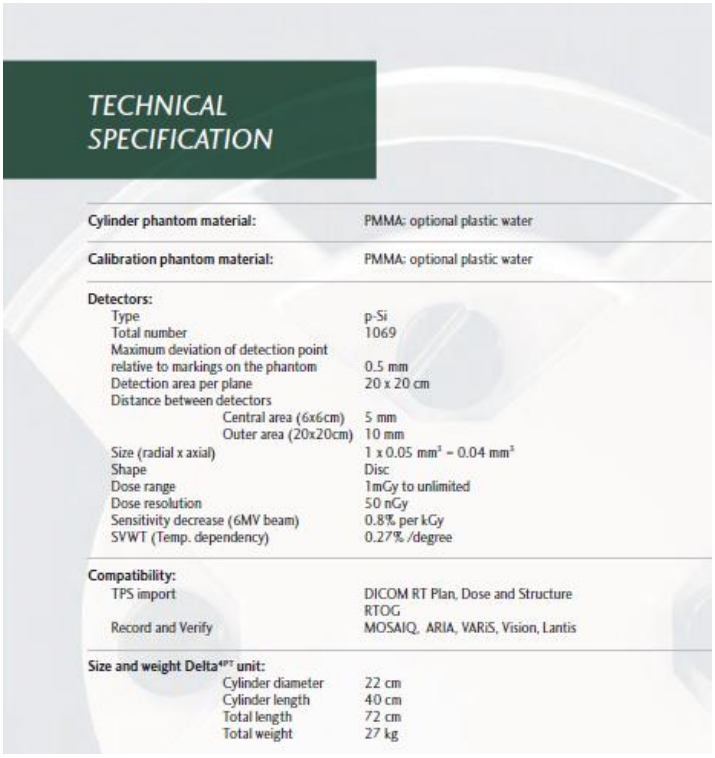

TECHNICAL SPECIFICATION

Cylinder phantom material:	PMMA: optional plastic water
Calibration phantom material:	PMMA: optional plastic water
Detectors:	
Type	p-Si
Total number	1069
Maximum deviation of detection point relative to markings on the phantom	0.5 mm
Detection area per plane	20 x 20 cm
Distance between detectors	
Central area (6x6cm)	5 mm
Outer area (20x20cm)	10 mm
Size (radial x axial)	1 x 0.05 mm^3 – 0.04 mm^3
Shape	Disc
Dose range	1mGy to unlimited
Dose resolution	50 nGy
Sensitivity decrease (6MV beam)	0.8% per kGy
SVWT (Temp. dependency)	0.27% /degree
Compatibility:	
TPS import	DICOM RT Plan, Dose and Structure RTOG
Record and Verify	MOSAIQ, ARIA, VARiS, Vision, Lantis
Size and weight Delta^{4PT} unit:	
Cylinder diameter	22 cm
Cylinder length	40 cm
Total length	72 cm
Total weight	27 kg

Technical specifications for the Scandidos Delta$^{4®}$ diode array.